

Pressure impulses generated by bubbles interacting with ambient perturbation

MIE ICHIHARA^a, and TAKESHI NISHIMURA^b

^aEarthquake Research Institute, University of Tokyo, Tokyo, Japan

^bTohoku University, Sendai, Japan

Article Outline

Glossary

1. Definition of the Subject and Its Importance
2. Introduction
3. Elementary processes in dynamics of a bubble
4. Bubbly Magma in an Elastic Rock as a Pressure Source
5. Acoustic bubbles in Hydrothermal Systems
6. Future Directions
7. Bibliography
8. Acknowledgements

Glossary

Impulse

The word 'impulse' is used in many areas in different ways. In classical mechanics, the impulse is the integral of force with respect to time. It is also used to refer to a fast-acting force, which is often idealized by a step function or a delta function. In this text, it is used to represent any functional form of pressure increase, either static or transient, which can generate observable signals.

Magma, melt, liquid

Magma is a general name for molten rock. It is fluid but contains solid and gas inclusions in liquid matrix. The matrix in magma is silicate melt (which is often called just 'melt'), and that in a hydrothermal system is water.

Volatile

Volatile is compound in silicate melt. The major component is H₂O, of which concentration is 1-5 wt%

depending mainly on pressure and composition of the melt. It exsolves from melt and forms gas bubbles at relatively low pressure (ca.100 MPa corresponding to the litho-static pressure around several kilo-meters). The second major component is CO₂,. Although its concentration is usually several ppm, some kinds of melts may dissolve 3-30 wt% of CO₂ at several GPa.

Long period seismic events

Long-period (or very long-period) seismic events are dominant in the period from about 1 s to more than a few tens of seconds. These signals at volcanoes are considered to be generated by interaction or resonance between volcanic fluid and the surrounding medium.

Ground deformation

Ground deformation is often observed at volcanoes when magma chambers inflate or deflate. Such ground deformation is detected by geodetic measurements such as GPS, tilt or strain meters, and the deformations often continue for a few tens of minutes to days or even months.

Magma chamber

Magma chamber is a storage system of molten magma. It is generally hard to detect, but is probably located at from a shallow depth (ca.1 km) to a few tens of km beneath the volcanoes. The shape and size have not been confirmed yet, but it is usually assumed to be rather round and hundreds to thousands of meters in scale. A magma storage system which has a horizontal extent is called a sill, and one which has a vertical extent is called a dike.

Rectified diffusion and rectified heat transfer

Rectified diffusion is a mechanism which can push dissolved volatiles into bubbles in a sound field. Bubbles take in more volatiles during expansion than they discharge during contraction, mainly because of the following two non-linear effects. Firstly, during expansion the bubble radius becomes larger so that the bubble surface is also larger than the surface during contraction. Secondly, radial bubble expansion tangentially stretches the diffusion layer and sharpens the radial gradient of the volatile concentration in the diffusion layer, so that the volatile flux into the bubble. The mechanism also works to push heat into bubbles and enhances evaporation in a liquid-vapor system. The rectified diffusion and heat transfer have been known and studied in the mechanical and chemical engineerings.

Bubble collapse

When the bubble is compressed, oscillates, or loses its mass by diffusion or phase change, it contracts to a very small size and sometimes disappear. Bubble collapse indicates the contraction of a bubble and does not necessarily indicate its disappearance.

1 Definition of the Subject and Its Importance

A volcano consists of solids, liquids, gases, and intermediate materials of any two of these phases. Mechanical and thermo-dynamical interactions of these phases are essential in generating variety of volcanic activities. In particular, the gas phase is mechanically distinct from the other phases and plays important roles in dynamic phenomena of volcanoes. When we work on volcanic activities, we are almost certainly confronted with physics problems associated with bubbles.

The roles of bubbles in volcanic activities have been investigated mainly in three aspects. Firstly, nucleation, growth, and expansion of bubbles are considered to be the main force that brings the magma to the surface [87, 62]. Secondly, a single bubble, if it is sufficiently large, may generate seismic waves when it rapidly expands or accelerates in the volcanic conduit [95, 81, 13, 34], and may generate acoustic waves in the air when it oscillates or bursts at the magma surface [94, 95, 84, 36]. Thirdly, existence of bubbles can significantly reduce the sound velocity [16, 42] and increase attenuation and dispersion of the waves [30, 44, 15]. This effect is considered to be relevant to many spectral features of seismic waves and air-waves associated with volcanic activities [10, 3, 22, 45].

Studies on bubble dynamics relevant to the volcanology are spread over many research fields and cannot be covered by a single paper. Good review papers and textbooks have already been published on bubble phenomena in sound fields [70, 73, 72, 61] and on nucleation and growth of bubbles in magma [62]. In this paper, we discuss several bubble dynamics phenomena selected from a particular point of view that the bubbly fluid works as an impulse generator. Here 'impulse' means a pressure increase, either static or transient, which can generate any observable signal (e.g. earthquakes, ground deformations, airwaves, and an eruption itself). Especially, we focus on the processes that the impulse is excited by non-linear coupling between internal processes of a bubbly fluid and an external perturbation. The importance of these processes have recently become noticed as a possible triggering mechanism of eruptions, earthquakes, and inflation of a volcano [57, 64]. Although it is generally considered that stress perturbation caused by preceding events is important, exact mechanisms to generate pressure increase which is required to trigger the subsequent events are yet under discussion.

In the first place, factors controlling a single bubble dynamics are summarized as the elementary processes in the bubbly fluid. Then two distinct liquid-bubble systems are considered, both of which are included in a volcano. The one is a body of bubbly magma confined in an elastic chamber, where elasticity of the

chamber, melt viscosity, and gas diffusion are important. The other is a hydrothermal system, where bubble oscillation, evaporation, and heat transfer are important.

2 Introduction

Elementary processes in a single-bubble dynamics

Radial motion of a single bubble interacting with ambient pressure perturbation is the elementary process controlling behaviors of the liquid-bubble mixtures. Although it appears quite simple, it contains various mechanisms in plenty. The great variety of behaviors of a single bubble has attracted many scientists, among which is Leonardo da Vinci [75]. Now results are used and studies are continued in many academic and industrial areas such as mechanical engineering, chemical engineering, medical science, and earth science.

Factors which may control the radial motion of a bubble are the pressure difference between inside and outside of the bubble, inertia and stress associated with deformation of the surrounding liquid, propagation of pressure waves, heat and mass transport, phase transition at the bubble wall, chemical reactions, relative translational motion between the bubble and the liquid, and so on. Because including all these mechanism at the same time to calculate a behavior of a bubble is unrealistic, we need to make adequate simplification and assumptions. Each mechanism has its own characteristic time scale in which the effect is dominant, and its own effect on the bubble dynamics. Knowing the individual time scales and features is important, when we want to understand and simulate a certain phenomenon correctly and efficiently. A brief review of some representative mechanism with linearized analyses are presented in section 3 for this purpose. Based on the results, geophysical phenomena and proposed models are discussed in the latter sections.

Bubbly Magma in an Elastic Rock as a Pressure Source

We consider a body of bubbly magma confined in an elastic rock. Pressure perturbations to the system are caused by change of tectonic stress due to local earthquakes, surface unloading by dome collapse, passing seismic waves from a near or distant source, depressurization of the chamber by degassing or magma leakage. Dynamic response of the system may be relevant to subsequent activities of the volcano as follows.

Nishimura [64] investigated pressure re-equilibration between the bubbles, the melt, and the surrounding elastic medium. It is assumed that the pressure of the system is suddenly decreased. After re-equilibration the original magma pressure is partially or completely recovered or even exceeded, depending on the size of the bubbles, stiffness of the elastic container, and the confining pressure. His model is used to explain rapid pressurization of a magma chamber triggered by lava-dome collapse at Soufriere Hills Volcano [96], and pressure recovery in a magma filling the chamber after explosive degassing to continue activities at Popocatepetl Volcano [11]. Shimomura et al. [86] extended the formulation of [64] to calculate the time profile

of the pressure recovery after sudden decompression. They showed that the time scale of the pressure recovery is strongly controlled by the system parameters, which include stiffness of the elastic container, bubble number density, diffusivity of the volatile in the melt, ambient pressure, and properties of the melt. Chouet et al. [12] also calculated the time profile assuming the system parameters for Popocatepetl Volcano, and compared the results with a particular source time function of a very-long-period seismic signal. Furthermore, in the same year, Lensky et al. [53] independently developed a mathematically equivalent model considering magma with CO₂ bubbles in mantle rock. They interpreted the results as a possible pressurization mechanism to initiate dikes in mantle which allows fast transport of magma.

There are in fact quite a few documented cases in which eruptions were triggered by local tectonic earthquakes (e.g. [47, 68]), and wave propagation from a distant earthquake (e.g. [8, 54]). Recently, Manga and Brodsky [57] have given a comprehensive review on the phenomena and possible mechanisms. Brodsky et al. [8] investigated a possibility that a strain wave from a distant earthquake can increase the pressure in a bubbly magma by rectified diffusion, which is a mechanism by which volatiles are pumped into a bubble by cyclic expansion and contraction. However, it has turned out that the mechanism by itself can cause negligibly small pressure increase [8, 29]. Several other mechanisms for long-range triggering have been proposed, which include pressure increase from rising bubbles [55], sub-critical crack growth [6], and fracture unclogging [7].

Acoustic Bubbles in Hydrothermal System

A hydrothermal system is another major source of pressure increase, long-period volcano seismic events [46], and triggered seismicity [57, 88]. Behaviors of a single bubble and liquid-bubble mixtures in a hydrothermal system are quite different from those in a magmatic system, mainly because of the water viscosity which is smaller than that of magma by more than several orders. We introduce several phenomena which are particular to the hydrothermal systems in section 5.

Geyser activity is well known for intermittent activity of hot-water effusion. The effusion process looks quite similar to volcanic eruptions, and some geysers are characterized by regular interval time and duration, which are also recognized in particular types of eruptions and seismic activities. Consequently, the geysers have been widely studied using seismological and geophysical techniques, as well as field observations, not only for clarifying the mechanism of the geysers but also for understanding the volcanic activities (e.g., [43, 40, 39, 65]). Kedar et al. [40, 39] conducted a unique experiment at Old Faithful Geyser, Yellowstone. They measured pressure within the geyser's water column simultaneously with seismic measurements on the surface. The data demonstrated that the tremor observed at Old Faithful results from impulsive events in the geyser. The impulsive events were modeled by a collapse of a spherical bubble by cooling that occurred

when the water column reached a critical temperature. Their data are reviewed in section 5 in relation to other studies on the dynamics of gas and vapor bubbles.

3 Elementary processes in a single-bubble dynamics

Equation of Motion for the Bubble Radius

Motion of a bubble is in fact a fluid dynamical problem for the liquid surrounding the bubble. The simplest model describing the behavior of a bubble is based on three assumptions: (1) the bubble is spherical, (2) the liquid is incompressible, and (3) the motion is radial. Using the basic equations of fluid mechanics, which are the continuity equation and the momentum equation, and the force balance at the bubble surface, the first equation of motion for the bubble radius was obtained by Rayleigh [79]:

$$\rho_l \left(R\ddot{R} + \frac{3}{2}\dot{R}^2 \right) = p(R) - p_l, \quad (1)$$

where R is the bubble radius, ρ_l is the liquid density, $p(R)$ is the pressure in the liquid at the bubble surface, and p_l is the pressure in the liquid at a large distance from the bubble. Using equation (1), Rayleigh [79] solved the problem of the collapse of an empty cavity in a large body of liquid at a constant p_l and showed the characteristic collapse time is

$$\tau_c = R_o \sqrt{\rho_l / p_l}. \quad (2)$$

The time τ_c is called Rayleigh collapse time and is one of the most important time scale in the bubble dynamics.

Plesset [69] extended equation (1) including the effects of liquid viscosity and surface tension. The generalized Rayleigh equation for bubble dynamics is called Rayleigh-Plesset equation[70]:

$$\rho_l \left(R\ddot{R} + \frac{3}{2}\dot{R}^2 \right) = p_g - p_l - 4\eta_l \frac{\dot{R}}{R} - \frac{2\Sigma}{R}, \quad (3)$$

where η_l is the liquid viscosity, and Σ is the surface tension. Equation (3) is valid for a Newtonian liquid under conditions of negligible mass exchange at the bubble surface. A further generalized equation to which these two restrictions do not apply is [71]:

$$\rho_l \left(R\dot{u}_l + \frac{3}{2}u_l^2 \right) - J \left[2u_l + J \left(\frac{1}{\rho_g} - \frac{1}{\rho_l} \right) \right] = p_g - p_l + \int_R^\infty \frac{3\tau_{rr}}{r} dr - \frac{2\Sigma}{R}, \quad (4)$$

where u_l is the radial liquid velocity at the bubble surface, $J = \rho_l(u_l - \dot{R})$ is the outgoing mass flux through the bubble wall, ρ_g is the density of the gas in the bubble, and τ_{rr} is the normal radial stress. When the interfacial mass flux J vanishes, $u_l = \dot{R}$ as in the left-hand side of the original equation (3).

While the above equations consider a single bubble in an infinite melt, magmatic systems often contain bubbles with some finite spacing. Cellular models of packing which include a finite volume of melt in

interaction with each bubble have been employed for closely spaced bubbles [78]. When the elementary cell is represented by a sphere with an outer radius of S , the equation corresponding to (3) is [75]:

$$\rho_l \left[R\ddot{R} \left(1 - \frac{R}{S} \right) + \frac{3}{2} \dot{R}^2 \left(1 - \frac{4}{3} \frac{R}{S} + \frac{1}{3} \frac{R^4}{S^4} \right) \right] = p_g - p_l - 4\eta_l \frac{\dot{R}}{R} \left(1 - \frac{R^3}{S^3} \right) - \frac{2\Sigma}{R}. \quad (5)$$

Equation (5) agrees with (3) for $S \rightarrow \infty$.

When there is no transport of heat or mass between the liquid and the bubble, the pressure in the bubble is determined by the instantaneous bubble radius alone. Using the ideal gas approximation, we have

$$p_g R^{3\gamma} = p_{g_o} R_o^{3\gamma}, \quad (6)$$

where γ is the specific heat ratio, and the subscript o indicates the equilibrium value of the variable. Substituting (6) into (3) for p_g and linearizing the equation, we obtain a damped oscillator equation:

$$\ddot{X} + 2b_v \dot{X} + \omega_o^2 X = -\frac{p'_l}{\rho_l R_o^2}, \quad (7)$$

$$b_v = \frac{2\eta_l}{\rho_l R_o^2}, \quad (8)$$

$$\omega_o = \frac{1}{R_o} \sqrt{\frac{3\gamma p_{g_o} - 2\Sigma/R_o}{\rho_l}}, \quad (9)$$

where X and p'_l are defined by $R = R_o(1 + X)$ and $p_l = p_{g_o} - 2\Sigma/R_o + p'_l$, respectively. Equation (7) is useful to see the characteristic behaviors of a bubble and their time scales. The resonant frequency of the bubble is ω_o (rad.s⁻¹). When the second term in the left-hand side of (7) dominates the first one in the time scale of the resonant oscillation, namely when $\omega_o < b_v$, the resonant oscillation is damped. In case of a gas bubble with a radius of 10^{-3} m in magma ($\rho_l = 2500$ kgm⁻³) at 10 MPa ($p_{g_o} - 2\Sigma/R_o = 10^7$ Pa), the frequency ($\omega_o/(2\pi)$) is about 20 kHz. The oscillation is damped when the viscosity is larger than 160 Pa.s. This viscosity is relatively small for magma. According to these estimations, we see that the free oscillation of a bubble in magma is possible in limited cases that the viscosity is small and the bubble is large. We also see that the bubble oscillation is easily excited in water which has a viscosity about 10^{-3} Pa.s.

Liquid rheology

The shear rheology of the liquid surrounding the bubble is one of the controlling factors for the bubble dynamics. According to experimental results, magma has viscoelastic nature, which is the most simply represented by linear Maxwell model [98]. Then the normal radial stress τ_{rr} in equation (4) is related to the corresponding strain rate \dot{e}_{rr} by

$$\tau_{rr} = \mu_l \int_0^t \exp\left(-\frac{t-t'}{\tau}\right) \dot{e}_{rr} dt', \quad (10)$$

where μ_l is the shear elasticity and τ is the relaxation time. In the limit of $t \ll \tau$, Maxwell relation (10) is reduced to a linear elastic stress-strain relation as $\tau_{rr} = \mu_l e_{rr}$. While in the limit of $t \gg \tau$, it is reduced to

Newtonian viscous relation, that is a linear stress-strain rate relation as $\tau_{rr} = \mu_l \tau \dot{\epsilon}_{rr}$, where $\mu_l \tau$ corresponds to the Newtonian viscosity η_l .

Fogler and Goddard [21] first used the viscoelastic relation (10) in the generalized Rayleigh-Plesset equation (4) without mass flux, and demonstrated that the influence of the viscoelastic effects on the radial motion of a bubble is characterized by a dimensionless parameter called Deborah number $De = \tau/\tau_c$, which compares the relaxation time τ and Rayleigh collapse time τ_c defined in (2): the influence is large when $\tau \gg \tau_c$. Extending the formulation by Fogler and Goddard [21] to a cellular bubble, Ichihara [28] investigated characteristic behaviors of the bubble in magmatic conditions. It is shown that, the elastic oscillation of a bubble, which occurs in case of $\tau \gg \tau_c$, is in a frequency of order of MHz and with very small displacement of the bubble wall because of the large shear modulus of the magma.

Change of the bubble radius in magma is mainly controlled by the viscosity except in magma with very small viscosity in which the bubble oscillation is possible. Therefore, in most of the studies for bubble growth in magma, effects of liquid inertia and viscoelasticity are not considered, and equation (3) or (5) for Newtonian fluid is used with neglect of the left-hand-side terms representing the inertia [87, 78, 62, 2]. Barclay et al [2] analytically solved the problem of the viscosity-controlled bubble expansion for instantaneous decompression, and showed the characteristic expansion time is

$$\tau_v = \frac{3\eta_l}{4p_l}, \quad (11)$$

where p_l is the pressure in the liquid. The time τ_v is one of the most important time scale in the bubble dynamics in magma [2, 30], while the Rayleigh collapse time τ_c , which is controlled by the inertia, is important in low-viscosity fluids including hydrothermal systems.

Definition of the viscous expansion time corresponding to (11) is different depending on problems and literatures. The time scale of the entire expansion of a bubble for instantaneous decompression is represented by (11) using the reduced pressure for p_l [2]. Volumetric oscillation of a bubble in an acoustic field is prevented by the viscous resistance if the period is shorter than τ_v , in this case with the initial static pressure for p_l [30]. When the bubble expansion is driven by a constant gas pressure, which occurs at the initial stage of diffusion-drive gas expansion when the gas is efficiently supplied from the liquid, the bubble grows approximately as $R \sim R_o \exp[t\Delta p/(4\eta_l)]$ [92, 62], where Δp is the pressure difference. In this case, $\tau_v = 4\eta_l/\Delta p$. The last case is discussed again later in the section of mass transport.

Liquid Compressibility

The effect of liquid compressibility on radial motion of a bubble was first considered in connection with underwater explosions [14, 41]. Liquid compressibility allows energy transport as a pressure wave so that it

causes radiation damping. Noting that the effect is considerable in case of a violent oscillation or collapse of a bubble, several mathematical approaches were proposed to include the effect in the equation of bubble radius. According to mathematical and numerical studies by Prosperetti and Lezzi [77], which compared the proposed equations, the following Keller's equation [41] is widely accepted as the most adequate form.

$$\rho_l \left[\left(1 - \frac{\dot{R}}{c_l}\right) R \ddot{R} + \frac{3}{2} \left(1 - \frac{\dot{R}}{3c_l}\right) \dot{R}^2 \right] = \left(1 + \frac{\dot{R}}{c_l} + \frac{R}{c_l} \frac{d}{dt}\right) \left(p_g - p_l - 4\eta_l \frac{\dot{R}}{R} - \frac{2\Sigma}{R}\right), \quad (12)$$

where c_l is the sound speed in the liquid. Although Prosperetti and Lezzi [77] further proposed to use the liquid enthalpy at the bubble wall instead of the pressure for the best accuracy, equation (12) is generally used in literatures.

Comparing (12) and (3), we can see that the correction terms due to the liquid compressibility have the order of \dot{R}/c_l . It means that the correction is considerable only when the bubble wall velocity becomes as large as the sound speed of the liquid. By applying $[1 + (\dot{R}/c_l) + (R/c_l)d/dt]^{-1}$ to both sides of (12) and linearizing the equation, Prosperetti [74] derived the acoustic damping coefficient, which corresponds to b_v in (8) for the viscous damping, as b_{ac} :

$$b_{ac} = \frac{\omega^2 R_o}{2c_l}, \quad (13)$$

where ω is the angular frequency of the oscillation. The acoustic damping is the more significant when the bubble is the larger and the oscillation frequency is the higher.

Effects of liquid compressibility on bubble dynamics in a highly viscous liquid are not understood comprehensively. Derivation of (12) and the related studies were performed thinking of liquids with ordinary viscosities like water. Therefore, the Reynolds number $Re = \rho_l R_o c_l / \eta_l$ was presupposed to be large. On the other hand, the viscosity of magma can be large enough to make Re very small. In this case, the same mathematical approximation is not necessarily applicable. Yamada et al. [99] pointed out this problem and solved the equations including viscous force associated with volumetric strain rate. Although the equation of motion for the bubble radius appears not to be affected by the compressibility when the system is initially hydrostatic, the velocity field around the bubble is different from the incompressible solution, even if the wall velocity is much smaller than the acoustic velocity.

There is arguments whether the equation of radial motion of a bubble surrounded by a finite volume of liquid needs correction terms for the compressibility. However, it seems to be negligible in magma, which is evaluated as follows [28]. In case that the bubble is surrounded by an elastic shell, contribution of the compressibility to the bubble expansion is $\delta_c R = R_o (p_g - p_l) (1 - R_o^3/S_o^3)^{-1} (3K_l)^{-1}$, where K_l is the bulk modulus of the liquid, which is the reciprocal of the compressibility [48]. We can evaluate $\delta_c R/R_o < 10^{-3}$, because $K_l \sim 10^{10} - 10^{11}$ Pa for magma [98], the realistic pressure difference, $p_g - p_l$ is not much larger than 10^7 Pa, and the volume fraction of the bubbles, R_o^3/S_o^3 , is reasonably assumed to be smaller than the

close-packing limit (~ 0.74). The change of p_g due to $\delta_c R$ is $\delta_c p_g / p_{go} \sim -3\delta_c R / R_o$, which is also in the same order. When the shell deforms viscously, displacement due to non-volumetric deformation grows, while that from the volumetric deformation remains in the same order.

Heat and Mass Transport

Each equation of motion for the bubble radius includes p_g , which is the pressure of the gas in the bubble, as we see in (3), (5), and (12). Equation (6) is available to calculate p_g only for an adiabatic process. In fact, when a bubble expands, the pressure and temperature in the bubble decreases. Then heat and volatile components flow into the bubble from the surrounding liquid. The opposite occurs when a bubble shrinks. The internal processes which control p_g are schematically shown in Figure 1. These transport effects are essential in most of actual systems including magmatic and hydrothermal systems.

Growth of a bubble by the mass diffusion in an over-saturated liquid is one of the fundamental problem. Based on purely dimensional considerations, an approximate growth law is given by

$$R\dot{R} = \frac{\kappa_{gl}\rho_l(C_o - C_{eq})}{\rho_g}, \quad (14)$$

where κ_{gl} is the diffusivity of the volatile in the liquid, C_o is the dissolved volatile concentration at a large distance from the bubble, and C_{eq} is the equilibrium concentration at the given pressure [70, 62]. From (14) we find that, asymptotically, $R \sim \sqrt{2\kappa_{gl}\rho_l(C_o - C_{eq})t/\rho_g}$. This expression is not valid at $t \rightarrow 0$ making $\dot{R} \rightarrow \infty$. In the initial stage, the diffusion is very efficient and the bubble growth is controlled by viscous resistance [92, 62]. In this stage, $R \sim R_o \exp[t\Delta p/(4\eta_l)]$ as discussed in the section of liquid rheology. The approximate time of the transition from the viscosity-controlled exponential solution to the diffusion-controlled square-root solution is found by Navon and Lyakhovsky [62] to be

$$\tau_{vd} \sim [-15 - 10 \log(Pe)]\eta_l/\Delta p, \quad (15)$$

where $Pe = \Delta p R_o^2 \eta_l^{-1} \kappa_{gl}^{-1}$ is Pecret number that compares the time scales of viscous expansion and diffusion. It is noted that equation (15) is validated for $Pe < 10^{-2}$, that is for relatively large viscosity and small bubble radius [62]. If we consider $\Delta p \sim 10^6$ Pa and $\kappa_{gl} \sim 10^{-11}$ m²s⁻¹, this condition is satisfied when $R_o^2 \eta_l^{-1} < 10^{-19}$, that is $\eta_l > 10^7$ Pa.s when $R_o \sim 10^{-6}$ m, and $\eta_l > 10^9$ Pa.s when $R_o \sim 10^{-5}$ m. Then the corresponding times are $\tau_{vd} > 50$ s and $\tau_{vd} > 5000$ s, respectively. Lensky et al. [51] have suggested that the change of the characteristic behavior of the bubble expansion over the time scale τ_{vd} generates a non-linear response of the liquid-bubble mixture to the pressure perturbation, which may cause amplification of a pressure wave. Coupling of effects of viscosity and diffusion on the bubble expansion also occurs through the material properties, because magma viscosity and water diffusivity are strongly influenced by the amount of dissolved water, which is the major volatile component in magma [50, 4].

Matsumoto and Takemura [60] numerically solved a complete set of equations for the radial dynamics of a bubble including conservation equation for mass, momentum, and energy in the bubble, heat and mass diffusion in the liquid, and heat and mass exchange between the gas and the liquid by diffusion and evaporation/condensation. Except in extremely rapid phenomena as the cases they treated, approximation of a spatially uniform pressure in the bubble is adequate [74]. With this approximation, the computational load is considerably reduced [63, 38, 9]:

It is necessary to consider non-uniform temperature distribution and compositions, in order to quantify the amounts of energy exchange between the bubble and liquid and energy loss associated with the non-equilibrium process. Time scales required to recover uniform temperature and composition in the bubble are controlled by diffusion processes and are much longer than that to attain uniform pressure, which is controlled by the pressure wave propagation in the bubble. Assuming representative values of the thermal diffusivity, $\kappa_T \sim 10^{-5}$ (m^2s^{-1}), and the inter-diffusivity of the components in the gas phase, $\kappa_{gi} \sim 10^{-7}$ (m^2s^{-1}) [38], development of thermal and material diffusion layers all over the bubble with radius of 10^{-3} m takes ~ 0.1 s and ~ 10 s, respectively. The time range of 0.1 -10 s is exactly what studies on seismoacoustic phenomena in volcanology are mainly concerned with. It takes even longer time to recover uniform concentration of volatile components in the liquid around the bubble. Therefore approximation of uniform temperature and compositions are not always adequate.

Again we introduce results from the linearized theory for a periodic acoustic field. The bulk modulus of a bubble, K_g , is defined as:

$$K_g = -\frac{R}{3} \frac{\partial p_g}{\partial R}, \quad (16)$$

which is generally a complex number. The elasticity and the energy loss associated with volumetric change of a bubble are represented by the real and imaginary parts of K_g , respectively. Then the damping factor and the resonant frequency for the bubble oscillation, which correspond to (8) and (9), respectively, are [74]:

$$b_t = \frac{3\text{Im}(K_g)}{2\rho_l\omega R_o^2} \quad (17)$$

$$\omega_o = \frac{1}{R_o} \sqrt{\frac{3\text{Re}(K_g) - 2\Sigma/R_o}{\rho_l}}. \quad (18)$$

In case of an adiabatic process for an ideal gas, where equation (6) holds, $K_g = \gamma p_{g_o}$ and (18) agree with (9). While in case of an isothermal process, $K_g = p_{g_o}$. In these two extreme conditions, $\text{Im}(K_g) = 0$ and there is no thermal damping.

In order to include the effect of non-uniform temperature distribution in the bubble, we have to solve the energy equation with the continuity of temperature at the bubble surface. Assuming that the pressure in the bubble is uniform, the temperature at the bubble wall is constant, which is supported by the large heat

capacity of the liquid compared with that of the gas, and the pressure perturbation is periodic ($\propto e^{i\omega t}$), the effective bulk modulus, K_g , is represented as [74]:

$$\frac{p_{go}}{K_g} = \frac{1}{\gamma} - \frac{3(\gamma-1)}{\gamma} i\chi \left[\sqrt{\frac{i}{\chi}} \coth \left(\sqrt{\frac{i}{\chi}} \right) - 1 \right], \quad (19)$$

$$\chi = \frac{\kappa_T}{\omega R^2}. \quad (20)$$

When the mass transfer is controlled by the diffusion of the volatile component in the liquid phase, the diffusion equation in the liquid and the equilibrium condition at the bubble surface are added. Then the effective bulk modulus which includes both the heat and mass transport is

$$\frac{p_{go}}{K_g} = \frac{1}{\gamma} - \frac{3(\gamma-1)}{\gamma} i\chi \left[\sqrt{\frac{i}{\chi}} \coth \left(\sqrt{\frac{i}{\chi}} \right) - 1 \right] - 3A_g \sqrt{\alpha_g} i\chi \left(\sqrt{\frac{i}{\chi}} + \sqrt{\alpha_g} \right), \quad (21)$$

$$A_g = \frac{\rho_l p_{go}}{\rho_{go}} \frac{\partial C_{eq}}{\partial p}, \quad (22)$$

$$\alpha_g = \frac{\kappa_{gl}}{\kappa_T}, \quad (23)$$

where C_{eq} is the saturation concentration at p_{go} [30]. Equation (21) has the last term in addition to (19), which represents the effect of the mass transfer. The dimensionless parameter, A_g , represents the ratio of the volatile mass going into the gas phase from a unit volume of the liquid phase by decompression to the mass change in a unit volume of the gas phase due to expansion.

Figure 2 shows the relevant range of the dimensionless parameters, A_g and α_g , for an H₂O bubble in magma [30]. As temperature decreases or pressure increases, A_g decreases (Figure 2) because of the following two reasons. With decreasing temperature, ρ_{go}^{-1} decreases. In case of magma, $C_{eq}(p)$ is approximately proportional to \sqrt{p} [26] so that $\partial C_{eq}/\partial p$ decreases with increasing pressure.

The effective bulk modulus of a bubble for some selected values of the parameters in the range is presented in Figure 3 [30]. The thick broken lines in the figure are obtained by (19), which includes only the heat transport. In this case, the real part approaches the isothermal bulk modulus and the adiabatic one in the low and high frequencies, respectively. The mass transport makes the bubble stiffness ($\text{Re}(K_g)$) smaller, which is the more significant in the lower frequency regime. It is because the bubble has more time to take in and out the volatile from the liquid in a cycle of the pressure perturbation.

The imaginary part for each parameter set has a local peak around

$$\omega \sim \tau_T^{-1} = 15\kappa_T R_o^{-2}, \quad (24)$$

which is the characteristic frequency of the energy loss due to heat transfer. In case of $R_o = 10^{-3}$ (m) and $\kappa_T = 4 \times 10^{-6}$ (m²s⁻¹), which is the value for H₂O at 10 MPa and 1273 K [5], the corresponding frequency ($\omega/(2\pi)$) is 9.5 Hz. The imaginary part of K_g including the diffusion effect has another peak at

the characteristic frequency of the energy loss due to the mass transport. The frequency is approximately represented by

$$\omega \sim \tau_g^{-1} = 9\alpha_g\kappa_T A_g^2 R_o^{-2}, \quad (25)$$

which is usually smaller than τ_T^{-1} [30]. It is noted that the above model assumes a single bubble in an infinite liquid. When the oscillation period is very long, interaction of the diffusion layers of the adjacent bubbles has to be considered [15].

When the mechanism of the mass exchange between the liquid and the bubble is the evaporation/condensation at the bubble wall, the latent heat plays an important role. Then the thermal diffusion equation in the liquid and the balance between the heat flux through the bubble surface and generation of the latent heat should be added [19, 24]. The corresponding bulk modulus of the bubble is represented as [24]:

$$\frac{p_{g0}}{K_g} = \frac{1}{\gamma} - \frac{3(\gamma-1)}{\gamma} \left(1 - \frac{c_{pg}T_o}{L}\right)^2 i\chi \left[\sqrt{\frac{i}{\chi}} \coth\left(\sqrt{\frac{i}{\chi}}\right) - 1 \right] - 3A_v \sqrt{\alpha_T} i\chi \left(\sqrt{\frac{i}{\chi}} + \sqrt{\alpha_T} \right), \quad (26)$$

$$A_v = \frac{\rho_l c_{pl} T_o p_{g0}}{(\rho_{g0} L)^2}, \quad (27)$$

$$\alpha_T = \frac{\kappa_{Tl}}{\kappa_T}, \quad (28)$$

where c_{pg} and c_{pl} are the heat capacity at constant pressure in the gas and the liquid phases, respectively, L is the latent heat, and κ_{Tl} is the thermal diffusivity in the liquid. In obtaining equation (26), the Clausius-Clapeyron relation: $(dp/dT)_{sat} = L\rho_g/T$, and thermodynamic relations for an ideal gas are used.

Equation (26) has the same form as (21) except $c_{pg}T_o/L$. This difference is due to the temperature change at the bubble wall. The dimensionless parameter, A_v , corresponds to A_g and has a similar physical meaning, which represents the ratio of the mass going through the phase change in a unit volume of the liquid phase to the mass change in a unit volume of the gas phase due to expansion. Although the equation is similar, the possible range of the parameter is different (Figure 2). As a result, the frequency dependence of K_g is also different as is shown in Figure 4. Comparing the figure with Figure 3, we can see that the energy loss of the vapor bubble due to the phase change is significant in a frequency range higher than that due to diffusion. The frequency range is comparable with that of the heat transfer, but the amount of energy loss is much larger. The vapor bubble loses its elasticity, which is represented by $\text{Re}(K_g)$, in the lower frequency as well.

Under the action of the sound field, there is a net transport of heat into the bubble by a non-linear process called rectified heat transfer [97]. In the evaporation/condensation system, the order of the non-linear effect is so large that it affects the amplitude and damping of the oscillation in the linear regime [24]. Equation (26) does not include the effect. Some works investigating the effect of rectified diffusion process in triggering an eruption or an earthquake are introduced in the later sections.

Translational Motion

So far we have neglected the translational motion of a bubble relative to the liquid. The translational motion is considered to be considerable when the displacement is comparable or larger than the diffusion layer in the liquid surrounding the bubble. In an acoustic field with frequency ω , this condition is represented by $U/\omega < \sqrt{\kappa/\omega}$, where U is the translational speed and κ is the relevant diffusivity. The translational velocity of a spherical bubble driven by buoyancy is estimated by $U = k\rho_l R_o^2 g \eta_l^{-1}$, where g is the gravitational acceleration. Although $k = 1/3$ for a pure liquid, $k = 2/9$ is used for most of actual liquid, which is not perfectly pure, because the pro-surface components concentrate on the bubble surface to make the surface less mobile[49]. These approximation hold for relatively slow velocity, which satisfies $Re_t = 2\rho_l R_o U \eta_l^{-1} \leq 1$. Then the condition in which the translational motion has a minor effect on the heat and mass transfer is

$$\omega > \frac{R^4}{\kappa} \left(\frac{k\rho_l g}{\eta_l} \right)^2. \quad (29)$$

Assuming $k = 2/9$, $R = 10^{-3}$ (m), $\kappa = \kappa_{gl} = 10^{-11}$ (m²s⁻¹), $\rho_l = 2500$ (kgm⁻³), $\eta_l = 10^5$ (Pa.s) for a magma-H₂O system, $\omega > 3 \times 10^{-4}$ (rad.s⁻¹) and $U = 6 \times 10^{-6}$ (m.s⁻¹). For water-vapor system, on the other hand, we assume $k = 1/3$, $\kappa = \kappa_{Tl} = 10^{-7}$, $\rho_l = 1000$, $\eta_l = 10^{-3}$. Then, if $R = 10^{-5}$, $\omega > 1$ and $U = 3 \times 10^{-4}$, and if $R = 10^{-4}$, $\omega > 10^4$ and $U = 3 \times 10^{-2}$. According to these estimations, we can see that the translational motion is negligible for most of cases with magma except basalt, which has relatively small viscosity ($\eta_l < 10^2$) and large diffusivity ($\kappa_{gl} \sim 10^{-9}$), while it is considerable in hydrothermal systems except for very small bubbles and the time scale is very short. As an example, the effect on thermal collapse of a vapor bubble is introduced later.

Another effect of the translational motion is its mechanical coupling with the radial motion. Because a bubble has to move the surrounding liquid in order to make itself move, it is subject to the inertial force of the liquid, which depends on its volume [49]. Therefore when the bubble volume changes, the force also changes. According to this consideration, an equation of the translational motion of the bubble is approximately represented as [100]:

$$\dot{U} = -\frac{3}{R}\dot{R}U + 2g - \frac{3}{4}\frac{C_D}{R}|U|U, \quad (30)$$

where C_D is the non-dimensional drag coefficient, which is given as a function of Re_t .

From the first term in the right-hand side, we see that the translational motion is decelerated by the bubble expansion. Although it had been theoretically recognized for long time, it was quantitatively justified by experiments recently [66]. The effect of the translational motion on the radial motion is represented with a term, $\rho U^2/2$. This term can usually be neglected [37, 66] except in cases with very strong oscillation [17].

4 Bubbly magma in an Elastic Rock as a Pressure Source

Model Overview

Here we consider a magma chamber filled with compressible viscous melt and numerous tiny H₂O gas bubbles (Figure 5) [78, 86]. The magma chamber is confined in an elastic rock. When perturbation is given to the system, pressure may increase by interaction of the elastic deformation of the chamber, expansion of the bubbles, and gas diffusion from the melt to the bubble. Recently, the process has been discussed in several literatures in relation to the observed volcanic phenomena [64, 86, 53, 12, 96, 8, 29], which are presented in Introduction.

The melt and bubbles are expressed by the cell model [78], in which multiple spherical bubbles of a constant radius are uniformly packed. Each bubble is surrounded by a finite volume of the melt, represented by an elementary cell. The elementary cell is spherical, in which a single gas bubble located at the center. It is assumed no interaction between neighboring elementary cells such that all gas bubbles grow in the same manner. This simplification enables us to examine bubble growth processes in the entire chamber by studying the growth of just a single bubble, which is represented by equation (5).

The main mechanism to increase the pressure is diffusion of the volatile. It is the slowest process of the bubble dynamics as is described in the previous section. It is certainly longer than the period of resonant oscillation of the individual bubbles so that the inertia terms in (5) are neglected. It is also longer than the time scale of the heat transport within the bubble as is shown in Figure 3 so that we may assume uniform and constant temperature within the bubble. Then the mathematical model for the elementary cell consists of three equations, which represent radial motion of the bubble, volatile diffusion in the melt, and ideal gas approximation, respectively, and three boundary conditions, which are phase equilibrium and mass flux at the bubble surface and no mass flux at the external boundary of the cell element.

Interaction Between Melt and Elastic Medium

The volumetric change of the bubbles and the melt due to the pressure change is compensated by the elastic deformation of the chamber. Here we consider the initial pressure and stress conditions in relation to physical process which brings about the condition, since the relations have not always been mentioned clearly in the previous literatures. We assume quasi-static deformation of the chamber, where the pressure of the melt is balanced by the elastic stress applied by the wall of the chamber. The volumetric change can be caused by (a) pressure change within the chamber and (b) stress change in the surrounding rock (Figure 6). Each process is individually represented by

$$p_l - p_o = \bar{\mu}_p \delta V_p / V_o, \quad (31)$$

$$-\sigma_\infty = \bar{\mu}_e \delta V_e / V_o, \quad (32)$$

where V_o is the initial equilibrium volume of the chamber, σ_∞ is the ambient stress change, δV_p and δV_e are the volumetric change due to (a) and (b), respectively, and $\bar{\mu}_p$ and $\bar{\mu}_e$ are corresponding effective stiffness of the wall. Each effective stiffness depends on the elasticity of the rock, the geometry of the chamber, and the applied stress field. For the simplicity, we approximate $\bar{\mu}_p = \bar{\mu}_e = \bar{\mu}$. Then the total volumetric change, δV , is given by

$$p_l - p_o - \sigma_\infty = \bar{\mu} \delta V / V_o, \quad (33)$$

The two perturbations to cause the volumetric change have not been clearly distinguished in the previous literatures. The mathematical treatment by [86] assumed that $p_l - p_o = -\Delta p$ is given at $t = 0$. They considered that this pressure drop is caused by decrease of the ambient stress field by a certain amount, say $\sigma_\infty = -\Delta\sigma$. On the other hand, the assumption of [12] is that the pressures in all of the bubble, the melt, and the rock are lower by Δp than the saturation pressure for the dissolved volatile concentration at $t = 0$. Strictly, the consequent processes are different depending on what causes the pressure perturbation. If the pressure drop of Δp occurred firstly within the chamber, that is $p_l - p_o = -\Delta p$ and $\sigma_\infty = 0$, the chamber would initially shrink according to (33). If it is caused by ambient stress drop first, that is $p_l - p_o = 0$ and $\sigma_\infty < 0$. Then the chamber would initially expand. In either case, the initial response is almost instantaneous, which is controlled by elasticity of the rock and compressibility of the melt. The major deformation occurs later and is controlled by volumetric change of the bubbles.

Response to Sudden Decompression and Characteristic Time for Pressure Recovery

There are three important parameters to characterize the response of the system to the pressure drop, which are useful for comparing the model and the field observations. The first one is the re-equilibrated pressure p_f . The second is the final bubble radius, R_f . The third is the characteristic time of the recovery process, T_{growth} .

The first and the second are calculated by consideration of the equilibrium condition alone and can be calculated semi-analytically [64]. On the other hand, T_{growth} is determined by numerical calculation of the set of equations described above. Shimomura et al. [86] investigated the recovery processes and presented that T_{growth} depends on the stiffness of the chamber ($\bar{\mu}$), initial bubble radius (R_o), number density of the bubbles (N), volatile diffusivity in the melt (κ_{gl}), initial pressure (p_o), the pressure drop (Δp), and the melt properties in a complicated manner.

The corresponding study for the bubble growth in an open space, where the pressure is constant regardless of the bubble expansion, was presented by Prousevitch et al.[78]. They assumed an initially supersaturated

condition, in which both p_{lo} and p_{go} are lower than the saturation pressure of the volatile dissolved in the melt. They investigated the final bubble radius and the time to reach it, which correspond to R_f and T_{growth} , respectively. They also presented effects of initial bubble radius (R_o), number density of the bubbles (N), volatile diffusivity in the melt (κ_{gl}), initial pressure (p_o), and initial super-saturation.

A simple theory to estimate the time scale of re-equilibration is useful to compare the model with observations, but has not been determined yet. Here we test two hypotheses.

1. The recovery time is comparable with the time scale in which the diffusion layer develops over the entire shell, that is $\tau_1 = (S_f - R_f)^2 / \kappa_{gl}$.
2. Based on a dimensional analysis of the simplified diffusion equation (14), Lensky et al. (2006) proposed $\tau_2 = (R_f^2 / \kappa_{gl})(\rho_{gf} / \rho_l)(C_o - C_f)^{-1}$, where ρ_{gf} and C_f are the final gas density in the bubble and the volatile concentration remained in the melt, both of which are functions of p_f . They obtained this equation based on the approximation that the quasi-static mass flux through the interface is $(C_o - C_{eq}(p_g)) / R$.

The re-equilibration times, T_{growth} , obtained by Shimomura et al. [86] and Prousevitch et al. [78] are compared with the above models in Figure 7. Comparing $T_{growth} - \tau_1$ (black symbols) and $T_{growth} - \tau_2$ (white symbols), we see that the general trend of T_{growth} is better estimated by τ_1 than by τ_2 in both confined and open systems. However, it should also be noted that τ_1 still has systematic errors which are indicated by gray frames. The errors are more dominant in the confined system (Figure 7a). It is indicated that the simple estimation does not include all the factors relevant to the re-equilibration time and it is not necessarily applicable to the wider range of the parameters.

Re-equilibration processes

Here we discuss different re-equilibration process depending on the cause of the pressure drop and the relevant initial conditions. Three representative solutions are presented in Figure 8-Figure 10. They are obtained for the standard basaltic system [86], but only viscosity is varied from 50 Pa.s for (a) to 10^6 Pa.s for (b).

Figure 8 is the case in which the stress drop occurs in the ambient rock first. It is generated by, for example, surface unloading by dome collapse [96] and stress change after a local earthquake. The condition is represented by $\sigma_\infty = -\Delta\sigma$ at $t \geq 0$ while $p_l = p_g - 2\Sigma/R_o = p_o$ at $t = 0$. According to (33), the chamber expands instantaneously, and p_l drops by Δp . Then the initial condition assumed by [64, 86] is attained. Response of p_g is not instantaneous [62]. Due to the difference between p_g and p_l , the bubble expands according to (5) to decrease p_g . Then difference between p_g and the equilibrium pressure for the volatile

concentration in the melt occurs to make the volatile flow into the bubble to re-increase p_g . As the bubbles grow, the entire volume of the magma (δV) increases to enlarge the chamber elastically. Then the elastic stress $\bar{\mu}\delta V/V_o$ increases p_l according to (33). The re-equilibration proceeds in this way [86].

Figure 9 is the case in which the pressure in the bubble as well as those in the melt and the ambient rock is lower than the saturation pressure for the initial volatile concentration in the melt at $t = 0$. This condition occurs, if bubbles are mixed with the super-saturated melt instantaneously or the bubbles are kept in the supersaturated mixture without interaction and suddenly allow the diffusion. Mathematically, the initial condition is equivalent to those assumed by [12] and [78]. The condition is represented by $p_l - p_o = p_g - 2\Sigma/R_o - p_o = \sigma_\infty = -\Delta p$ at $t \geq 0$. Diffusion of the volatile into the bubble starts, which increases p_g first. Then $p_g - p_l$ expands the bubble and the chamber to increase p_l in the same way as the previous case. Practically, the difference between Figure 8 and Figure 9 occurs only in the very short period in the beginning, and the subsequent increase of the pressure and volume of the chamber may look the same from outside.

Figure 10 is the case in which the pressure drop occurs in the melt and in the bubble, while the stress in the ambient rock is unchanged. The condition is represented by $p_l - p_o = p_g - 2\Sigma/R_o - p_o = -\Delta p$ and $\sigma_\infty = 0$. Although the assumed initial condition is rather imaginary, this case is presented in order to demonstrate how the response can be different depending on the way the system is 'decompressed'. In fact, it is more realistic that p_l drops first, while p_g remains at the initial value. This situation may occur by small leakage of the melt from the system. In this case, the melt pressure just recovers almost instantaneously, because the container compresses the melt according to (33) and bubbles also compress the melt. No other significant change is expected. On the other hand, if both p_l and p_g drop, as in Figure 10, the pressure still recovers rapidly, but bubbles are compressed. Because the mechanical balance of the bubble and the melt is attained with $p_g - 2\Sigma/R = p_l$ according to equation (5), p_g has to become larger when R decreases. Then p_g exceeds the equilibrium pressure for the volatile in the melt to make the volatile dissolve into the melt.

Rectified Diffusion

So far, we discussed responses of the system to a stepwise pressure drop. When the perturbation is caused by a seismic wave from an external source, the system is subject to a cyclic disturbance. Rectified diffusion is a mechanism which can push dissolved volatiles into bubbles in a sound field. Bubbles take in more volatiles during expansion than they discharge during contraction, mainly because of the following two non-linear effects [27, 18]. Firstly, the interface is larger during expansion than during contraction. Secondly, radial bubble expansion tangentially stretches the diffusion layer and sharpens the radial gradient of the volatile concentration in the diffusion layer, so that the volatile flux into the bubble is enhanced.

Brodsky et al. [8] discussed the possible pressure increase of a bubbly magma confined in an elastic rock by this mechanism. Using the solution by Hsieh and Plesset [27] for a periodic system, they considered that, even though the net pressure changes are determined by the pre-existing oversaturation, the rectified diffusion accelerates the pressure increase and may break the balance which had been stabilized the system prior to the oscillation. Ichihara and Brodsky [29] improved the solution by including resorption of gas as the pressure increase and development of the diffusion layer around the bubble in a self-consistent way. It is then shown that rectified diffusion is not faster than the ordinary diffusion and its contribution to the net pressure change is at the most 2×10^{-9} of the initial pressure regardless of the pre-existing oversaturation.

5 Acoustic bubbles in Hydrothermal Systems

Pressure Impulses Generated in a Geysers

Here we consider a mixture of water and vapor bubbles, in which we expect effects of bubble oscillations and evaporation.

Kedar et al. [40, 39] conducted field experiments at Old Faithful Geysers, Yellowstone. They measured pressure within the geysers' water column simultaneously with seismic measurements on the surface. The data show a distinct cause-and-effect relationship between the impulsive pressure source and the impulse response of the rock surrounding the water column. In addition, the pressure pulse, which is strongest at the top transducer, strongly attenuates downward. Considering that the pulse is generated by the oscillation of a single bubble, they compared one selected signal with a solution of the equation of motion for the bubble radius (3). In order to fit the measured oscillation with a reasonable bubble radius, they had to assume a very small ambient pressure to lower the frequency, and a very large viscosity to increase the damping. For $R_o = 0.055$ m, for example, they used $p_{go} = 0.02$ MPa, with which equation (9) gives the resonant frequency close to the observation: ~ 20 Hz. The viscosity was assumed as $\eta_l = 40$ Pa.s, which is larger than the actual value by more than four orders. They compared the damping coefficient with those from radiation and heat transfer, though these effects were not included in the calculation of (3), and concluded that mechanisms other than acoustic, thermal, or viscous damping are required to explain the strong damping observed.

We have already introduced the damping coefficient b_t with the evaporation effect in equations (17) with (26). Then, assuming the similar bubble radius and frequency ranges as [39], let us see the damping coefficient by evaporation in comparison with the other coefficients, which are for viscous, acoustic and thermal damping, represented by (8), (13), and (17) with (19), respectively. Their values are compared in Figure 12b, assuming $p_{go} = 0.13$ MPa (the saturation pressure at 380 K). We can see that the evaporation effect significantly increases the damping and dominates the other damping mechanisms in the frequency range of the geysers oscillation. The evaporation effect also decreases $\text{Re}(K_g)$ (Figure 12a) in the range. It is

thus suggested that the evaporation effect is significant for the bubble dynamics in the hydrothermal system.

Inertial and Thermal Collapse of a Bubble

When we heat water in a kettle, we hear strong intermittent pulses before boiling starts. The phenomenon is explained in terms of the bubble dynamics as follows [1]. In the first regime (which initiates above approximately 40 °C) small bubbles form slowly out of dissolved air in the liquid, rising silently to the surface as they break off the side of the vessel. At higher temperature (~ 70 °C), vapor bubbles start to nucleate at various sites at the heated bottom surface of the container. Vapor bubbles are different from the air bubbles in that their formation and collapse (at the bottom of the vessel) occurs explosively, producing pressure impulses that traverse the liquid and excite many of the sound we hear. In the third stage (between 90 °C and 100 °C), vapor bubbles grow, coalesce, and survive their ascent through the liquid. Bursting of vapor bubbles at the top surface is considered to be the sound source in this regime. Finally, the transition to full boil is characterized by large bubble formation throughout the bulk of the liquid.

We consider whether and how the impulse generation by the bubble collapse occurs in a geyser, where water that is already boiling is injected and cooled from the surface [43]. The collapse (or growth) of a bubble is classified into two modes: the inertia mode, which is controlled by the liquid inertia and driven by the pressure difference between the liquid and the bubble, and the thermal mode, which is controlled by the heat transfer and driven by the temperature difference [102, 20]. The former is more violent than the latter and is responsible for the impulse generation.

Based on theoretical and experimental studies, Florschuetz and Chao [20] proposed that the relative importance of the inertia and the heat transfer is evaluated by a dimensionless parameter, B , defined by

$$Ja = \frac{\rho_l c_{pl}(T_{sat}(p_{lo}) - T_o)}{\rho_{go} L}, \quad (34)$$

$$B = Ja^2 \frac{\kappa T_l}{R_o} \sqrt{\frac{\rho_l}{p_{lo} - p_{sat}(T_o)}}, \quad (35)$$

where $T_{sat}(p_{lo})$ is the saturation temperature for the ambient pressure (p_{lo}) and $p_{sat}(T_o)$ is the saturation pressure for the system temperature (T_o). The dimensionless parameter Ja is called Jacob number, which represents the degree of subcooling. Figure 13 is their calculation results, which clearly shows that for $B \geq 0.3$, the collapse rate is dominated by liquid inertia effect, while for $B \leq 0.03$, it is much slower and is recognized as the thermal mode. For an intermediate value of B , oscillation is observed.

In these works [76, 20], it is often assumed that the pressure in the bubble is initially equal to the saturation pressure of the subcooled liquid, that is $p_{go} = p_{sat}(T_o)$, which is smaller than the ambient pressure (p_{lo}) [20, 76]. Experimentally, it is achieved by preparing for a thermally equilibrium water-vapor system at a low pressure and suddenly increasing the system pressure to p_{lo} [20]. Then the initial collapse

is relatively violent and continues by inertia until the vapor heating at the bubble wall increase the vapor pressure above the ambient pressure to such an extent that the liquid is momentarily brought to rest and its motion actually reverses before the vapor pressure again drops below the system pressure [20, 76]. Although the oscillation is difficult to see on the radius change curves in Figure 13 for small B , the beginning inertia controlled stage is evidenced by that all the curves start along the inertia curve.

On the other hand, in case that a bubble suddenly enters cold water, $p_{go} = p_{lo} > p_{sat}(T_o)$ while temperature in the bubble T_{go} is larger than T_o and is close to $T_{sat}(p_{go})$. Then the collapse begins in the gentle mode controlled by the heat transfer. It can turn into the inertia mode only if the rate of heat transport and condensation to decrease the vapor pressure is so large that inward motion of the surrounding liquid cannot follow. Prosperetti and Hao [76] presented that relative translational motion between the bubble and the liquid significantly increases the rate of heat transport and accelerates the bubble collapse. Furthermore, they pointed out the coupling effect between the translational and the radial motions. As equation (30) suggests, the decreasing bubble radius ($\dot{R} < 0$) works to accelerates the translational motion. Although the drag force ($\propto C_D R^{-1} |U|U$) increases as R decreases and U increases, there are cases in which the contribution of the first term is so large to make $\dot{U} > 0$. Then the bubble collapse and the translational motion accelerate each other [76].

Rectified Heat Transfer

In the same way as the rectified diffusion discussed in the previous section, rectified heat transfer works for a vapor bubble in an acoustic field [97, 24]. When the bubble is compressed, some vapor condenses, the surface temperature rises, and heat is conducted away into the adjacent liquid. When the bubble expands during the following half cycle, evaporation causes a temperature drop of the bubble surface, with a consequent heat flux from the liquid. The imbalance of the heat flux and the interface area between the compression phase and the expansion phase causes the net energy flux into the bubble.

Sturtevant et al. [88] investigated the effect of rectified diffusion on pressure increase in a hydrothermal system, as a possible mechanism for triggered seismicity by a distant earthquake. They modeled the system as a two-component H_2O-CO_2 system, and considered rectified mass diffusion. As is mentioned in the previous section, the net pressure change due to rectified mass diffusion is very small, if it is evaluated in a self-consistent way [29].

Although rectified heat transfer has a similar mechanisms as the rectified mass transfer, it is much more intense since the thermal diffusivity of liquids typically exceeds the mass diffusivity by two orders of magnitude [76]. It can grow a vapor bubble quickly within several cycles of oscillation at the beginning (Figure 14), and thus can be effective even with low-frequency pressure waves. Moreover the effect is reinforced

by the coupling effect of the bubble growth and translational motion [25], and coupling of evaporation and diffusion of another gas component [38]. The net energy flux into the bubble increases the temperature in the bubble, which may change the liquid static pressure [24]. It is noted that numerical results in the literatures cannot be directly used to estimate the pressure increase, because they were obtained for an open system in which the bubble continues to grow instead of increasing system pressure. However, it might be worth to re-evaluate effects of rectified processes in a hydrothermal system taking account of these recent results.

Non-Linear Oscillation of a Spherical Cloud of Bubbles

Oscillation of a group of bubbles generates particular signals as well as oscillation of a single bubble. The presence of bubbles can lower the acoustic speed of the fluid by an order of magnitude [42, 16], if the liquid viscosity is small enough [31, 30]. Therefore, there is a sharp impedance contrast between a region of bubbly liquid and a region of pure liquid. The boundary of a bubble cloud acts like an elastic boundary that traps acoustic energy in the bubbly region so that the bubble cloud has characteristic frequency of resonance [56, 101, 67]. Chouet [10] considered it is the mechanism for the harmonic oscillations observed at volcanoes having relatively low-viscosity magma. He showed the typical values for the oscillation in the few Hz range may be generated by a columnar bubble cloud with void fraction of 1 %, ~ 100 m in length, and ~ 1 m in radius in a bubble-free magma with ~ 5 m in radius. The radius of each bubble is assumed as 10^{-3} m, which has its own resonance frequency at 8.9 kHz [10].

Omta [67] conducted numerical calculation for oscillation of a spherical cloud of bubbles with relatively large amplitude. Figure 15 shows one of his results, in which the cloud oscillation was excited by an external pressure increase. Three cycles of the oscillation are presented. We can see high-frequency strong pulsation at the center of the bubble cloud (Figure 15a). It is explained as follows [67]. The pressure perturbation is amplified and sharpened toward the center of the cloud because of the spherical geometry. Then the bubbles are excited at their resonance frequency.

The strong pulsation is observed only near the center in a spherical bubble cloud (Figure 15). If a bubble cloud is hemispherical with its cross section attached on a solid wall, the pulsation generated at the center of the hemisphere may strongly hit the wall [85]. Generation of strong high-frequency pulses by a bubble cloud interacting with a pressure perturbation with lower frequencies is actually observed in experiments and now the phenomenon is going to be applied to medical treatment under controlled condition [33, 59]. Similar mechanism may work in a hydrothermal system, in which a low-frequency perturbation generates strong pressure impulses hitting the walls to be observed as seismic waves. In fact pressure oscillations in the bubble cloud (Figure 15) and in the geyser (Figure 11) have quite similar features, though their time

scales are different by three orders.

6 Future Directions

We have summarized theoretical bases of the bubble dynamics, mainly based on radial motion equations of a single bubble. These theories have been established and verified by experiments for simple systems. For volcanic systems, these theories have mainly been applied to the nucleation and growth of bubbles in magma. This subject takes an important part of volcanology, though it is not included in this review paper. By comparing the theory with observation of bubbles left in natural volcanic rock [93, 58] and re-producing the process by laboratory experiments [23, 89, 52], researchers have determined physical parameters of the volcanic processes, which are the temperature, pressure, volatile saturation, ascent rate, and so on. The bubble dynamics theories have also been applied to explain geophysical observations, as we have reviewed several possible mechanisms of bubbles that generate pressure impulses. However, determining the effects or even existence of bubbles is more difficult in these phenomena than in the bubble growth problems, because direct observation of bubbles and re-production of the process in a laboratory are more difficult. Here we discuss how we can go forward to confirm the models and apply them to determine useful physical parameters.

It would be effective to focus on relatively simple volcanic phenomena in which the bubble dynamics theory appears to work. Especially, for some volcanoes which make eruption frequently, data taken by modern geophysical methods are being accumulated and the phenomenological cause-and-result relations between an eruption and pressure impulses before and during the eruption are well documented. For example, at Stromboli volcano all the sequences of the repetitive small eruptions and a few proximal explosions have been taken by multi-parameter monitoring systems [83, 82]. Geophysical data taken close to active craters at Sakurajima, Suwanosejima, and Semeru volcanoes have revealed common features in the pressure change before and during an explosion [32]. At Sakurajima volcano, behaviors of a shallow gas pocket are discussed in the sequences of seismic and explosion events based on analyses of seismic data [91, 90]. It might be possible and useful to have a common backbone model for these eruptions, based on which we can explain the particular detail of each case as a result of different parameters of the system.

The bubble dynamics theory which is used in the models needs to be updated, too. Responses of a bubbly fluid are sensitive to the system parameters, which determine possibilities, features, and time scales of the individual mechanisms, as are shown in the text. Although many models assume uniform system for simplicity, the natural system is considered to be non-uniform. In other words, regions having different physical parameters may coexist. Interaction of these subsystems may enhance the characteristic response, but may diminish with one another, or generate completely different effects. The inhomogeneities

and their interactions may occur in various scales and manners. For example, in section 4, behaviors of a single uniform magma body in an elastic rock have been discussed. In the real system, the bubble size and the chemical composition are likely to be non-uniform within a small region and/or over the entire magma body. If the system is large, the hydrostatic pressure gradient is significant. Moreover, if there are plural magma containers which have different physical parameters, each magma body will respond to the pressure perturbation differently, and pressure gradient may be generated between the two adjacent containers. Developing a model including these subscale interactions may be a subject of modern multi-scale multi-physics studies.

Laboratory experiments using analogous materials are useful in verifying and improving the models. In the procedure to construct a model system, we frequently find factors which are important in the real system but have been neglected in the idealized mathematical model. Although there may be some processes which can be realized in the nature more easily, and there always be a scaling problem, experiments will give us more concrete idea about the mechanism of the models. Although most of the previous analogue experiments are designed to be compared with geological and petrological observations, there are some which investigate generation of pressure impulses by bubbles and are intended to explain seismic and/or acoustic observations [34, 35, 80]. According to the results and implications obtained by these preceding works, laboratory studies in this direction are promising.

It is also important to connect geophysical observation and geological data to understand the bubble dynamics phenomena in volcanology. Compared with other geophysical processes which occur in the earth, there is larger possibility that the source of activity appears to the surface after relatively short time. The geological samples (e.g., pyroclasts during eruptions and volcanic gasses) can inform us physical and chemical properties of the materials generating pressure impulses, and would make useful constraints on the model. On the other hand, these constraints can be tested and verified by geophysical signals of seismic, geodetic and acoustic measurements when the models are established.

By combining these theoretical, experimental, geophysical, and geological approaches, we will get better understanding on the processes which generate volcanic activities.

7 Acknowledgements

The authors are grateful to Dr. B. Chouet, and Dr. H. Kawashima for useful information and advise. We also thank to Dr. M. Kameda and two anonymous reviewers for their help to improve the manuscript.

References

- [1] Aljishi, S. and Tatarkievicz, J.: Why does heating water in a kettle produce sound ?, *Am. J. Phys.*, Vol. 59 (1991), 628–632.
- [2] Barclay, J., Riley, D. S. and Sparks, R. S. J.: Analytical models for bubble growth during decompression of high viscosity magmas, *Bull. Volcanol.*, Vol. 57 (1995), 422–431.
- [3] Benoit, J. P. and McNutt, S. R.: New constraints on source processes of volcanic tremor at Arenal Volcano, Costa Rica, using broadband seismic data, *Geophys. Res. Lett.*, Vol. 24 (1997), 449–452.
- [4] Blower, J. D., Mader, H. M. and Wilson, S. D. R.: Coupling of viscous and diffusive controls on bubble growth during explosive volcanic eruptions, *Earth Planet. Sci. Lett.*, Vol. 193 (2001), 47–56.
- [5] Bowers, T. S.: Pressure-volume-temperature properties of H₂O CO₂ fluids, in Ahrens, T. J. ed., *A Handbook of Physical Constants: Rock Physics and Phase Relations, AGU Reference Shelf Series 3*, AGU, 1995, 45–72.
- [6] Brodsky, E. E., Karakostas, V. and Kanamori, H.: A new observation of dynamically triggered regional seismicity: Earthquakes in Greece following the August, 1999 Izmit, Turkey earthquake, *Geophys. Res. Lett.*, Vol. 27 (2000), 2741–2744.
- [7] Brodsky, E. E., Roeloffs, E., Woodcock, D., Gall, I. and Manga, M.: A mechanism for sustained groundwater pressure changes induced by distant earthquakes, *J. Geophys. Res.*, (2003), 2390.
- [8] Brodsky, E. E., Sturtevant, B. and Kanamori, H.: Earthquakes, volcanoes, and rectified diffusion, *J. Geophys. Res.*, Vol. 103 (1998), 23827–23838.
- [9] Campos, F. B. and Lage, P. L. C.: Heat and mass transfer modeling during the formation and ascension of superheated bubbles, *Int. J. Heat Mass Transfer*, Vol. 43 (2000), 2883–2894.
- [10] Chouet, B. A.: New methods and future trends in seismological volcano monitoring, in Scarpa, R. and Tilling, R. eds., *Monitoring and Mitigation of Volcano Hazards*, Springer-Verlag, Berlin, Heidelberg, 1996, 23–97.
- [11] Chouet, B., Dawson, P. and Arciniega-Ceballos, A.: Source mechanism of Vulcanian degassing at Popocatepetl Volcano, Mexico, determined from waveform inversions of very long period signals, *J. Geophys. Res.*, Vol. 110 (2005), B07301.
- [12] Chouet, B., Dawson, P. and Nakano, M.: Dynamics of diffusive bubble growth and pressure recovery in a bubbly rhyolitic melt embedded in an elastic solid, *J. Geophys. Res.*, Vol. 111 (2006), B07310 doi:.

- [13] Chouet, B., Dawson, P., Ohminato, T. and Martini, M.: Source mechanisms of explosions at Stromboli Volcano, Italy, determined from moment-tensor inversions of very-long-period data, *J. Geophys. Res.*, Vol. 108 (2003), doi:.
- [14] Cole, R. H.: *Underwater Explosions*, Dover Pub. Inc., New York, 1948.
- [15] Collier, L., Neuberg, J. W., Lensky, N., Lyakhovsky, V. and Navon, O.: Attenuation in gas-charged magma, *J. Volcanol. Geotherm. Res.*, Vol. 153 (2006), 21–36.
- [16] Commander, K. W. and Prosperetti, A.: Linear pressure waves in bubbly liquid - comparison between theory and experiments, *J. Acoust. Soc. Am.*, Vol. 85 (1989), 732–746.
- [17] Doinikov, A. A.: Equations of coupled radial and translational motions of a bubble in a weakly compressible liquid, *Phys. Fluids*, Vol. 17 (2005), 128101 doi:10.1063/1.2145430.
- [18] Eller, A. and Flynn, H. G.: Rectified diffusion during nonlinear pulsations of cavitation bubbles, *J. Acoust. Soc. Am.*, Vol. 37 (1965), 493–503.
- [19] Finch, R. D. and Neppiras, E. A.: Vapor bubble dynamics, *J. Acoust. Soc. Am.*, Vol. 53 (1973), 1402–1410.
- [20] Florschuetz, L. W. and Chao, B. T.: On the mechanics of vapor bubble collapse, *Trans. ASME, J. Heat Transfer*, Vol. 87 (1965), 209–220.
- [21] Fogler, H. S. and Goddard, J. D.: Collapse of spherical cavities in viscoelastic fluids, *Phys. Fluids*, Vol. 13 (1970), 1135–1141.
- [22] Garces, M. A. and McNutt, S. R.: Theory of the airborne sound field generated in a resonant magma conduit, *J. Volcanol. Geotherm. Res.*, Vol. 78 (1997), 155–178.
- [23] Gardner, J. E., Hilton, M. and Carroll, M. R.: Experimental constraints on degassing of magma: isothermal bubble growth during continuous decompression from high pressure, *Earth Planet. Sci. Lett.*, Vol. 168 (1999), 201–218.
- [24] Hao, Y. and Prosperetti, A.: The dynamics of vapor bubbles in acoustic pressure fields, *Phys. Fluids*, Vol. 11 (1999), 2008–2019.
- [25] Hao, Y. and Prosperetti, A.: Rectified heat transfer into translating and pulsating vapor bubbles, *J. Acoust. Soc. Am.*, Vol. 112 (2002), 1787–1796.

- [26] Holloway, J. R. and Blank, J. G.: Application of experimental results to C-O-H species in natural melts, in Carroll, M. R. and Holloway, J. R. eds., *Volatiles in Magma, Rev. Miner., 30*, Mineral. Soc. Am., Washington, DC, 1994, 187–230.
- [27] Hsieh, D.-Y. and Plesset, M. S.: Theory of rectified diffusion of mass into gas bubbles, *J. Acoust. Soc. Am.*, Vol. 33 (1961), 206–215.
- [28] Ichihara, M.: Dynamics of a spherical viscoelastic shell: Implications to a criterion for fragmentation/expansion of bubbly magma, *Earth Planet. Sci. Lett.*, (2007), (in press).
- [29] Ichihara, M. and Brodsky, E. E.: A limit on the effect of rectified diffusion in volcanic systems, *Geophys. Res. Lett.*, Vol. 33 (2006), L02316.
- [30] Ichihara, M. and Kameda, M.: Propagation of acoustic waves in a visco-elastic two-phase system: influences of the liquid viscosity and the internal diffusion, *J. Volcanol. Geotherm. Res.*, Vol. 137 (2004), 73–91.
- [31] Ichihara, M., Ohkunitani, H., Ida, Y. and Kameda, M.: Dynamics of bubbly oscillation and wave propagation in viscoelastic liquids, *J. Volcanol. Geotherm. Res.*, Vol. 129 (2004), 37–60.
- [32] Iguchi, M., Tameguri, T. and Yakiwara, H.: Source Mechanisms of Volcanic Explosion Revealed by Geophysical Observations at Sakurajima, Suwanosejima and Semeru volcanoes, *Eos Trans. AGU*, Vol. 87 (2006), Abstract V31G–03.
- [33] Ikeda, T., Yoshizawa, S., Tosaki, M., Allen, J. S., Takagi, S., Ohta, N., Kitamura, T. and Matsumoto, Y.: Cloud cavitation control for lithotripsy using high intensity focused ultrasound, *Ultrasound in Med. & Biol.*, Vol. 32 (2006), 1383–1397.
- [34] James, M. R., Lane, S. J. and Chouet, B. A.: Gas slug ascent through changes in conduit diameter: Laboratory insights into a volcano-seismic source process in low-viscosity magmas, *J. Geophys. Res.*, Vol. 111 (2006), B05201.
- [35] James, M. R., Lane, S. J., Chouet, B. and Gilbert, J. S.: Pressure changes associated with the ascent and bursting of gas slugs in liquid-filled vertical and inclined conduits, *J. Volcanol. Geotherm. Res.*, Vol. 129 (2004), 61–82.
- [36] Johnson, J. B., Aster, R. C. and Kyle, P. R.: Triggering of volcanic eruptions, *Geophys. Res. Lett.*, Vol. 31 (2004), doi:.

- [37] Kameda, M. and Matsumoto, Y.: Shock waves in a liquid containing small gas bubbles, *Phys. Fluids*, Vol. 8 (1996), 322–335.
- [38] Kawashima, H., Ichihara, M. and Kameda, M.: Oscillation of a vapor/gas bubble with heat and mass transport, *Trans. JSME, Ser. B*, Vol. 67 (2001), 2234–2242.
- [39] Kedar, S., Kanamori, H. and Sturtevant, B.: Bubble collapse as the source of tremor at Old Faithful Geysers, *J. Geophys. Res.*, Vol. 103 (1998), 24283–24299.
- [40] Kedar, S., Sturtevant, B. and Kanamori, H.: The origin of harmonic tremor at Old Faithful geyser, *Nature*, Vol. 379 (1996), 708–711.
- [41] Keller, J. B. and Kolodner, I. I.: Damping of underwater explosion bubble oscillations, *J. Appl. Phys.*, Vol. 27 (1956), 1152–1161.
- [42] Kieffer, S. W.: Sound speed in liquid-gas mixtures: water-air and water-steam, *J. Geophys. Res.*, Vol. 82 (1977), 2895–2904.
- [43] Kieffer, S. W.: Geologic nozzles, *Rev. Geophysics*, Vol. 27 (1989), 3–38.
- [44] Kumagai, H. and Chouet, B. A.: Acoustic properties of a crack containing magmatic or hydrothermal fluids, *J. Geophys. Res.*, Vol. 105 (2000), 25493–25512.
- [45] Kumagai, H. and Chouet, B. A.: The dependence of acoustic properties of a crack on the resonance mode and geometry, *Geophys. Res. Lett.*, Vol. 28 (2001), 3325.
- [46] Kumagai, H., Chouet, B. A. and Nakano, M.: Temporal evolution of a hydrothermal system in Kusatsu-Shirane Volcano, Japan, inferred from the complex frequencies of long-period events, *J. Geophys. Res.*, Vol. 107 (2002), 2236.
- [47] La Femina, P. C., Connor, C. B., Hill, B. E., Strauch, W. and Saballos, J. A.: Magma-tectonic interactions in Nicaragua: the 1999 seismic swarm and eruption of Cerro Negro volcano, *J. Volcanol. Geotherm. Res.*, Vol. 137 (2004), 187–199.
- [48] Landau, L. D. and Lifshitz, E. M.: *Theory of Elasticity, 3rd Edition*, Butterworth-Heinemann, Oxford, 1986.
- [49] Landau, L. D. and Lifshitz, E. M.: *Fluid Mechanics, 2nd. Ed.*, Pergamon Press, Oxford, 1987.
- [50] Lensky, N. G., Lyakhovskiy, V. and Navon, O.: Radial variations of melt viscosity around growing bubbles and gas overpressure in vesiculating magmas, *Earth. Planet. Sci. Lett.*, Vol. 186 (2001), 1–6.

- [51] Lensky, N. G., Lyakhovsky, V. and Navon, O.: Expansion dynamics of volatile-supersaturated liquids and bulk viscosity of bubbly magmas, *J. Fluid Mech.*, Vol. 460 (2002), 39–56.
- [52] Lensky, N. G., Navon, O. and Lyakhovsky, V.: Bubble growth during decompression of magma: experimental and theoretical investigation, *J. Volcano. Geotherm. Res.*, Vol. 129 (2004), 7–22.
- [53] Lensky, N. G., Niebo, R. W., Holloway, J. R., Lyakhovsky, V. and Navon, O.: Bubble nucleation as a trigger for xenolith entrapment in mantle melts, *Earth. Planet. Sci. Lett.*, Vol. 245 (2006), 278–288.
- [54] Linde, A. T. and Sacks, I.: Triggering of volcanic eruptions, *Nature*, Vol. 395 (1998), 888–890.
- [55] Linde, A. T., Sacks, I., Johnston, M. J. S., Hill, D. P. and Bilham, R. G.: Increased pressure from rising bubbles as a mechanism for remotely triggered seismicity, *Nature*, Vol. 371 (1994), 408–410.
- [56] Lu, N. Q., Prosperetti, A. and Yoon, S. W.: Underwater noise emissions from bubble clouds, *IEEE J. Oceanic Eng.*, Vol. 15 (1990), 275–281.
- [57] Manga, M. and Brodsky, E.: Seismic triggering of eruptions in the far field: Volcanoes and geysers, *Ann. Rev. Earth Planet. Sci.*, Vol. 34 (2006), 263–291.
- [58] Mangan, M. T. and Cashman, K. V.: The structure of basaltic scoria and reticulite and inferences for vesiculation, foam formation, and fragmentation in lava fountains, *J. Volcanol. Geotherm. Res.*, Vol. 73 (1996), 1–18.
- [59] Matsumoto, Y., Allen, J. S., Yoshizawa, S., Ikeda, T. and Kaneko, Y.: Medical ultrasound with microbubbles, *Exp. Therm. Fluid Sci.*, Vol. 29 (2005), 255–265.
- [60] Matsumoto, Y. and Takemura, F.: Influence of internal phenomena on gas bubble motion (Effects of thermal diffusion, phase change on the gas-liquid interface and mass diffusion between vapor and noncondensable gas in the collapsing phase), *JSME Int. J., Ser. B.*, Vol. 37 (1994), 288–296.
- [61] Nakoryakov, V. E., Pokusaev, B. G. and Shreiber, I. R.: *Wave Propagation in Gas-Liquid Media, 2nd Edition*, CRC Press, Boca Raton, 1993.
- [62] Navon, O. and Lyakhovsky, V.: Vesiculation processes in silicic magmas, in Gilbert, J. S. and Sparks, R. S. J. eds., *The Physics of Explosive Volcanic Eruption*, Geol. Soc., London, Special Publications, 145, 1998, 27–50.
- [63] Nigmatulin, R. I., Khabeev, N. S. and Nagiev, F. B.: Dynamics, heat and mass-transfer of vapor-gas bubbles in a liquid, *Int. J. Heat Mass Trans.*, Vol. 24 (1981), 1033–1044.

- [64] Nishimura, T.: Pressure recovery in magma due to bubble growth, *Geophys. Res. Lett.*, Vol. 31 (2004), L12613.
- [65] Nishimura, T., Ichihara, M. and Ueki, S.: Investigation of the Onikobe geyser, NE Japan, by observing the ground tilt and flow parameters, *Earth Planets Space*, Vol. 58 (2006), e21–e24.
- [66] Ohl, C. D., Tijink, A. and Prosperetti, A.: The added mass of an expanding bubble, *J. Fluid Mech.*, Vol. 482 (2003), 271–290.
- [67] Omta, R.: Oscillations of a cloud of bubbles of small and not so small amplitude, *J. Acoust. Soc. Am.*, Vol. 82 (1987), 1018–1033.
- [68] Oura, A., Yoshida, S. and Kudo, K.: Rupture process of the Ito-Oki Japan earthquake of 1989 July 9 and interpretation as a trigger of volcanic-eruption, *Geophys. J. Int.*, Vol. 109 (1992), 241–248.
- [69] Plesset, M. S.: The dynamics of cavitation bubbles, *J. Appl. Mech.*, Vol. 16 (1949), 277–282.
- [70] Plesset, M. S. and Prosperetti, A.: Bubble dynamics and cavitation, *Ann. Rev. Fluid Mech.*, Vol. 9 (1977), 145–185.
- [71] Prosperetti, A.: A generalization of the Rayleigh-Plesset equation of bubble dynamics, *Phys. Fluids*, Vol. 25 (1982), 409–410.
- [72] Prosperetti, A.: Acoustic cavitation series: part three, Bubble phenomena in sound fields: part two, *Ultrasonics*, Vol. 222 (1984), 115–124.
- [73] Prosperetti, A.: Acoustic cavitation series: part two, Bubble phenomena in sound fields: part one, *Ultrasonics*, Vol. 222 (1984), 69–78.
- [74] Prosperetti, A.: The thermal behavior of oscillating gas bubbles, *J. Fluid Mech.*, Vol. 222 (1991), 587–616.
- [75] Prosperetti, A.: Bubbles, *Phys. Fluids*, Vol. 16 (2004), 1852–1865.
- [76] Prosperetti, A. and Hao, Y.: Vapor bubbles in flow and acoustic fields, *Ann. N. Y. Acad. Sci.*, Vol. 974 (2002), 328–347.
- [77] Prosperetti, A. and Lezzi, A.: Bubble dynamics in a compressible liquid, 1. 1st-order theory, *J. Fluid Mech.*, Vol. 168 (1986), 457–478.
- [78] Prousevitch, A. A., Sahagian, D. L. and Anderson, A. T.: Dynamics of diffusive bubble growth in magmas: Isothermal case, *J. Geophys. Res.*, Vol. 98 (1993), 22,283–22,307.

- [79] Rayleigh, L.: On the pressure developed in a liquid during the collapse of a spherical cavity, *Philos. Mag.*, Vol. 34 (1917), 94–98.
- [80] Ripepe, M., Ciliberto, S. and Della Schiava, M.: Time constraints for modeling source dynamics of volcanic explosions at Stromboli, *J. Geophys. Res.*, Vol. 106 (2001), 8713–8727.
- [81] Ripepe, M. and Gordeev, E.: Gas bubble dynamics model for shallow volcanic tremor at Stromboli, *J. Geophys. Res.*, Vol. 104 (1999), 10639–10654.
- [82] Ripepe, M., Marchetti, E., Poggi, P., Harris, A., Fiaschi, A. J. L. and Ulivieri, G.: Seismic, Acoustic and Thermal Network Monitors the 2003 Eruption of Stromboli Volcano, *EOS, Trans. AGU*, Vol. 85 (2004), 329.
- [83] Ripepe, M., Marchetti, E., Ulivieri, G., DelleDonne, D., Genco, R. and Lacanna, G.: Monitoring the 2007 Stromboli effusive eruption by an integrated geophysical network, *The 21st Century COE Earth Science International Symposium*, Vol. Abstracts (2007), 327–327.
- [84] Ripepe, M., Poggi, P., Braun, T. and Gordeev, E.: Infrasonic waves and volcanic tremor at Stromboli, *Geophys. Res. Lett.*, Vol. 23 (1996), 181–184.
- [85] Shimada, M., Matsumoto, Y. and Kobayashi, T.: Influence of the nuclei size distribution on the collapsing behavior of the cloud cavitation, *JSME Int. J. Ser. B*, Vol. 155 (2006), 307–322.
- [86] Shimomura, Y., Nishimura, T. and Sato, H.: Bubble growth processes in magma surrounded by an elastic medium, *J. Volcanol. Geotherm. Res.*, Vol. 155 (2006), 307–322.
- [87] Sparks, R. S. J.: Dynamics of bubble formation and growth in magmas - Review and analysis, *J. Volcanol. Geotherm. Res.*, Vol. 3 (1978), 1–37.
- [88] Sturtevant, B., Kanamori, H. and Brodsky, E. E.: Seismic triggering by rectified diffusion in geothermal systems, *J. Geophys. Res.*, Vol. 101 (1996), 25269–25282.
- [89] Suzuki, Y., Gardner, J. E. and Larsen, J. F.: Experimental constraints on syneruptive magma ascent related to the phreatomagmatic phase of the 2000AD eruption of Usu volcano, Japan, *Bull. Volcanol.*, Vol. 69 (2007), 423–444.
- [90] Tameguri, T., Iguchi, M. and Ishihara, K.: Mechanism of explosive eruptions from moment tensor analyses of explosion earthquakes at Sakurajima volcano, *Bull. Volcanol. Soc. Japan*, Vol. 47 (2002), 197–215.

- [91] Tameguri, T., Maryanto, S. and Iguchi, M.: Source mechanisms of harmonic tremors at Sakurajima volcano, *Bull. Volcanol. Soc. Japan*, Vol. 52 (2007), 273–279.
- [92] Toramaru, A.: Numerical study of nucleation and growth of bubbles in viscous magmas, *J. Geophys. Res.*, Vol. 100 (1995), 1913–1931.
- [93] Toramaru, A.: BND (bubble number density) decompression rate meter for explosive volcanic eruptions, *J. Volcanol. Geotherm. Res.*, Vol. 154 (2006), 303–316.
- [94] Vergnolle, S. and Brandeis, G.: Origin of the sound generated by Strombolian explosions, *Geophys. Res. Lett.*, Vol. 21 (1994), 1959–1962.
- [95] Vergnolle, S. and Brandeis, G.: Strombolian explosions .1. A large bubble breaking at the surface of a lava column as a source of sound, *J. Geophys. Res.*, Vol. 101 (1996), 20433–20447.
- [96] Voight, B., Linde, A. T., Sacks, I. S., Mattioli, G. S., Sparks, R. S. J., Elsworth, D., Hidayat, D., Malin, P. E., Shalev, E., Widiwijayanti, C., Young, S. R., Bass, V., Clarke, A., Dunkley, P., Johnston, W., McWhorter, N., Neuberg, J. and Williams, P.: Unprecedented pressure increase in deep magma reservoir triggered by lava-dome collapse, *Geophys. Res. Lett.*, Vol. 33 (2006), L03312.
- [97] Wang, T.: Rectified heat transfer, *J. Acoust. Soc. Am.*, Vol. 56 (1974), 1131–1143.
- [98] Webb, S. L.: Silicate melts: Relaxation, rheology, and the glass transition, *Rev. Geophys.*, Vol. 35 (1997), 191–218.
- [99] Yamada, K., Emori, H. and K., N.: Bubble expansion rates in viscous compressible liquid, *Earth Planets Space*, Vol. 58 (2006), 865–872.
- [100] Yang, B., Prosperetti, A. and Takagi, S.: The transient rise of a bubble subject to shape or volume changes, *Phys. Fluids*, Vol. 15 (2003), 2640–2648.
- [101] Yoon, S. W., Crum, L. A., Prosperetti, A. and Lu, N. Q.: An investigation of the collective oscillations of a bubble cloud, *J. Acoust. Soc. Am.*, Vol. 89 (1991), 700–706.
- [102] Zuber, N.: The dynamics of vapor bubbles in nonuniform temperature fields, *Int. J. Heat Mass Transfer*, Vol. 2 (1961), 83–98.

Table.1 List of important variables and constants.

Notation	Unit	Definition
C_{eq}	-	Equilibrium volatile concentration (weight fraction) in the liquid
c_l	m.s^{-1}	Sound speed in the liquid
c_{pg}	$\text{Jkg}^{-1}\text{K}^{-1}$	Heat capacity of the gas at constant pressure
c_{pl}	$\text{Jkg}^{-1}\text{K}^{-1}$	Heat capacity of the liquid at constant pressure
K_g	Pa	Effective bulk modulus of the bubble
K_l	Pa	Bulk modulus of the liquid
L	Jkg^{-1}	Latent heat
p_g	Pa	Pressure in the bubble
p_g	Pa	Pressure in the liquid far from the bubble
R	m	Bubble radius
S	m	Outer radius of the cellular bubble
T	K	Temperature
U	m.s^{-1}	Translational velocity of the bubble
γ	-	Specific heat ratio
η_l	Pa.s	Liquid viscosity
κ_{gl}	m^2s^{-1}	Diffusivity of the volatile in the liquid
κ_T	m^2s^{-1}	Thermal diffusivity in the bubble
κ_{Tl}	m^2s^{-1}	Thermal diffusivity in the liquid
$\bar{\mu}$	Pa	Effective stiffness of the magma chamber
μ_l	Pa	Shear elasticity of the liquid
ρ_l	kg.m^{-3}	Liquid density
Σ	m.s^{-1}	Surface tension
σ_∞	Pa	Ambient stress change given to the magma chamber
τ	s	Maxwell relaxation time
ω	rad.s^{-1}	Angular frequency

Table.2 List of characteristic times.

Notation	Equation	Definition
τ_c	(2)	Inertia-controlled bubble collapse
τ_g	(25)	Mass diffusion in the liquid around the bubble
τ_T	(24)	Thermal diffusion in the bubble
τ_v	(11)	Viscosity-controlled bubble expansion
ω_o	(9)	Natural frequency of a bubble

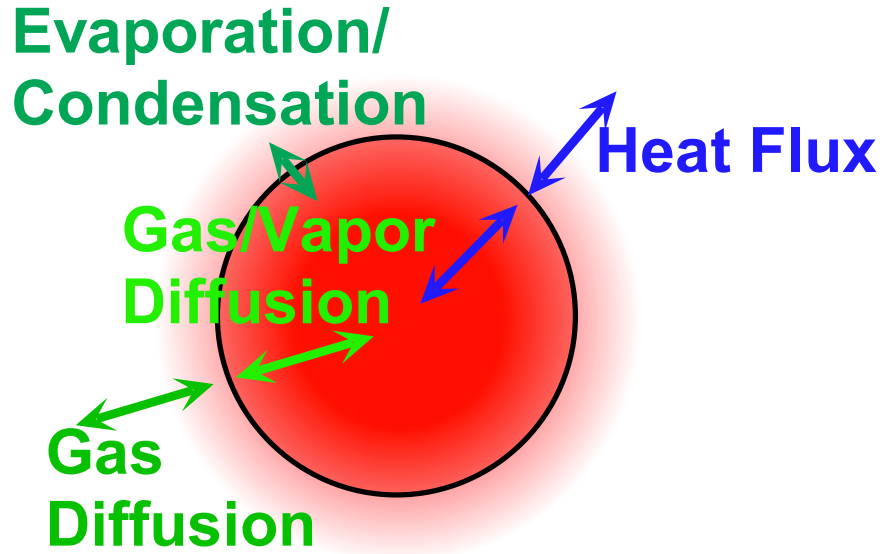


Figure 1: The internal heat and mass transport processes which control pressure change and energy loss associated with the bubble oscillation.

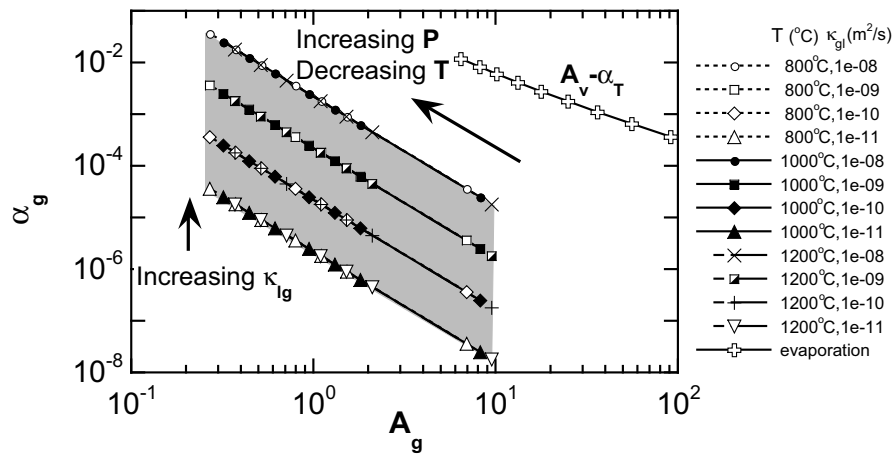


Figure 2: The relevant range of the dimensionless parameters representing the effect of the volatile transfer in the magmatic system is shown as the gray area. The parameter A_g and α_g are defined in eqs. (22) and (23), respectively. The temperature (T) and the volatile diffusivity (κ_{gl}) are assumed as shown in the legend, and the pressure is varied from 0.1 to 100 MPa. The open crosses are the corresponding parameters for a vapor-bubble system, A_v and α_T given in equations (27) and (28), respectively. The temperature is varied from 380 K to 500 K and the pressure is the saturation pressure at each temperature. (Modified from [30]Fig.1)

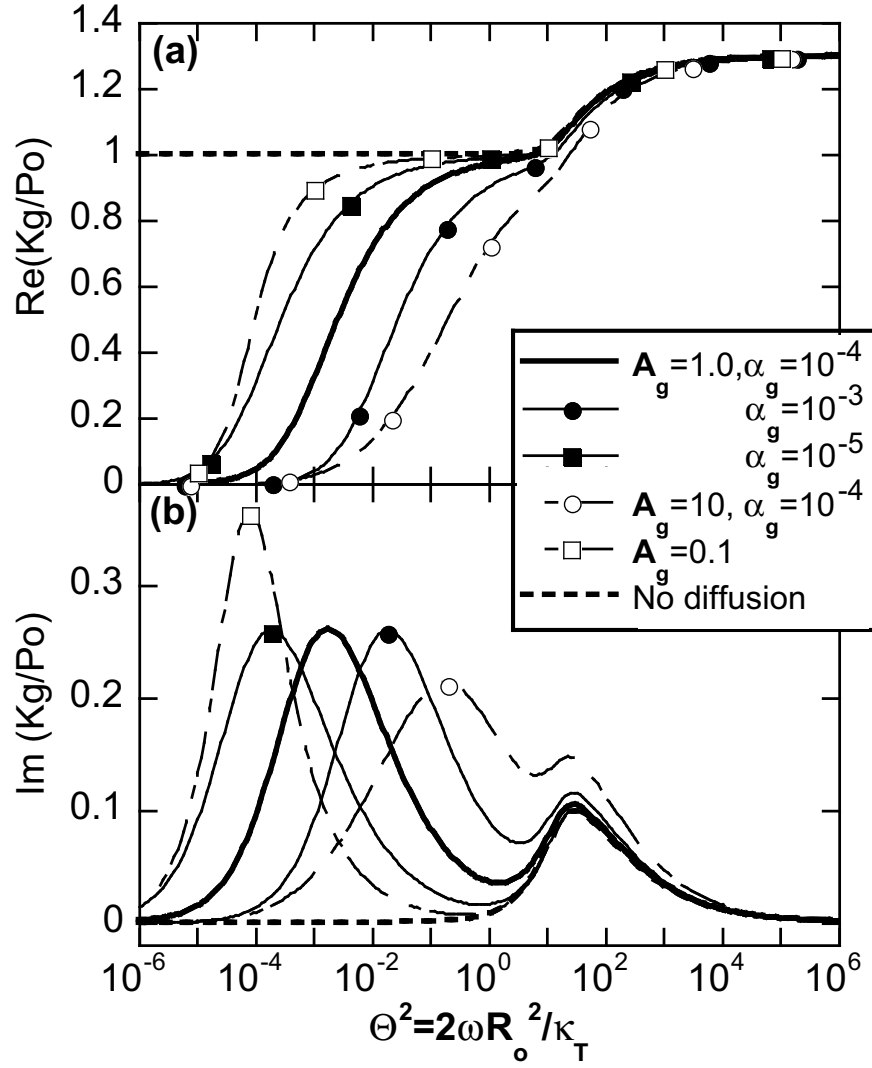


Figure 3: The effective bulk modulus of a gas bubble with heat and mass diffusion (calculated by equation (21)) as a function of the dimensionless frequency. The real and the imaginary parts are presented in (a) and (b), respectively. The thick broken lines indicated as 'No diffusion' includes only thermal effect (which is calculated by equation (19)). ([30] Fig.2)

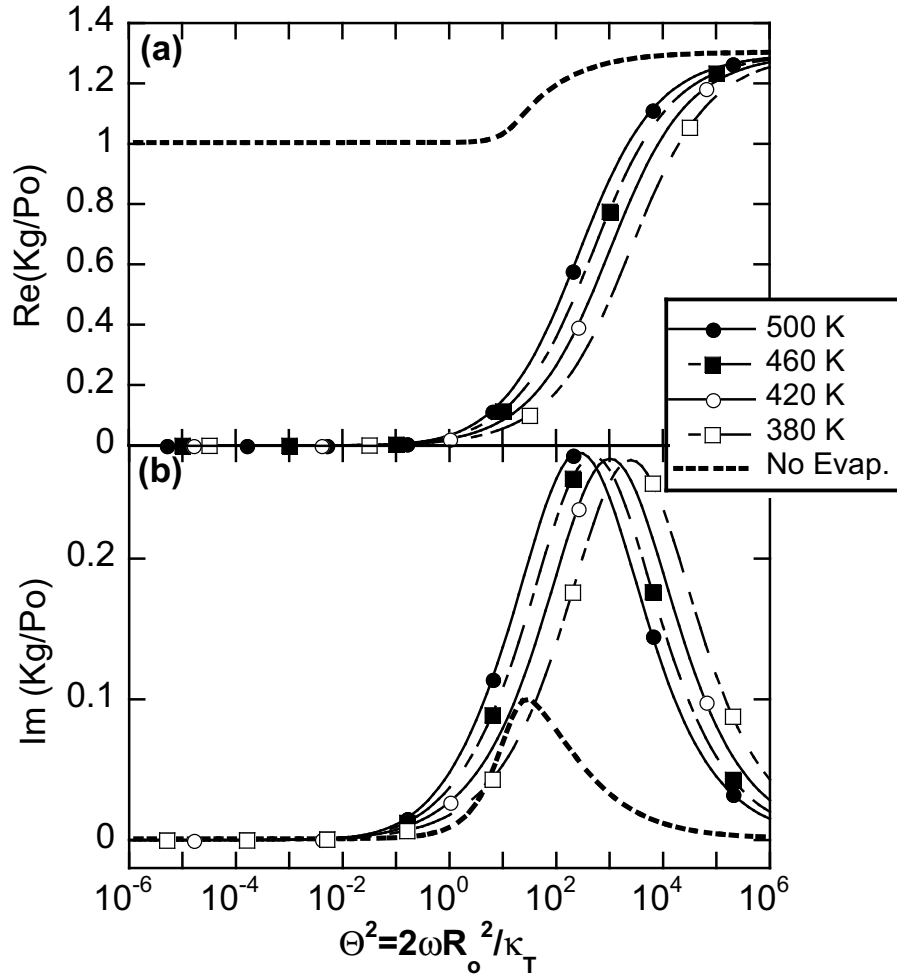
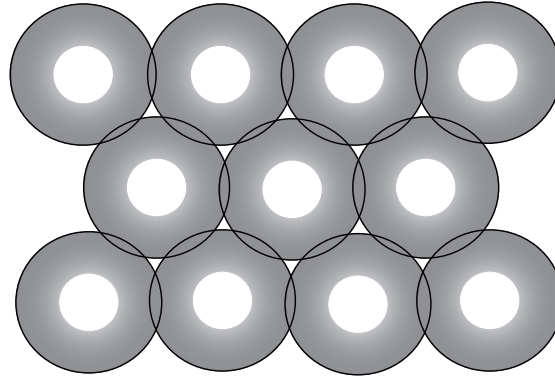
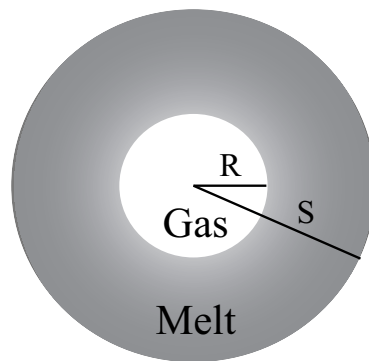


Figure 4: The effective bulk modulus of a vapor bubble with thermal and evaporation effects (calculated by equation (26)) as a function of the dimensionless frequency. The real and the imaginary parts are presented in (a) and (b), respectively. The thick broken lines indicated as 'No evaporation' includes only thermal effect (which is calculated by equation (19)).

a.



b.



c.

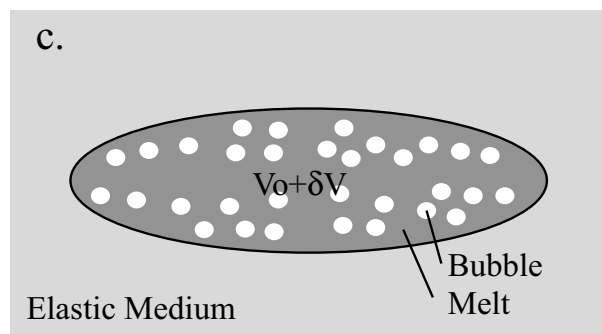


Figure 5: Schematic illustrations of (a) cell model [78], (b) an elementary cell, and (c) a chamber surrounded by an elastic medium. The chamber is filled with compressible viscous melt and numerous tiny spherical gas bubbles. Magma is represented by a combination of many elementary cells. R and S is the radius of the elementary cell and gas bubble, respectively, and $V_0 + \delta V$ is the volume of the chamber. (modified from [86]Fig.1)

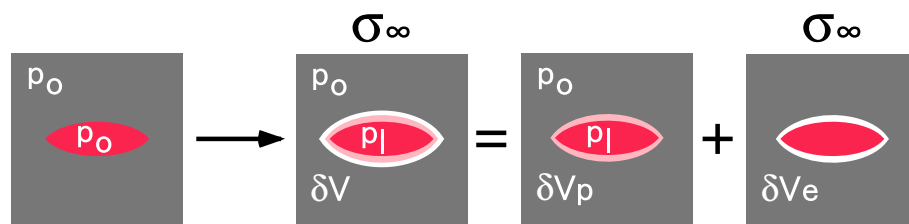


Figure 6: Mathematical for interaction of melt pressure p_l , stress in the ambient rock σ_∞ , and volume change of the chamber, δV . Volume change due to internal overpressure $p_l - p_o$ and that due to external stress is considered separately.

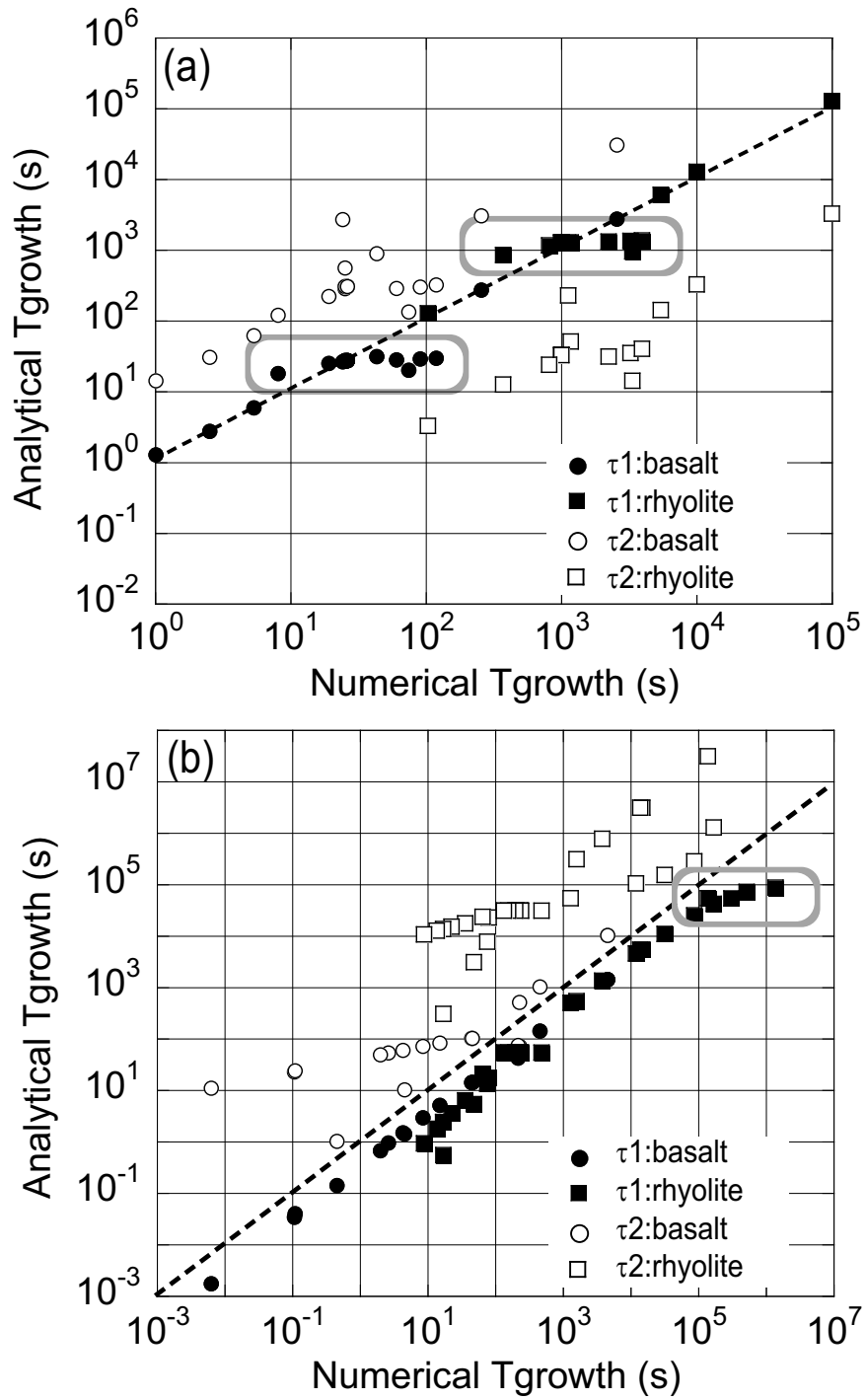


Figure 7: Numerical results of the pressure recovery time for magma in an elastic rock (a) and the bubble growth time in an open system (b) for various system parameters are compared with analytical approximations: τ_1 is the time scale of mass diffusion across the final shell thickness, τ_2 is approximation by [53]. Agreement between the numerical results and τ_1 is better, but some systematic discrepancy remains, as are indicated by gray frames. The numerical results for (a) is from [86], and those for (b) is from [78].

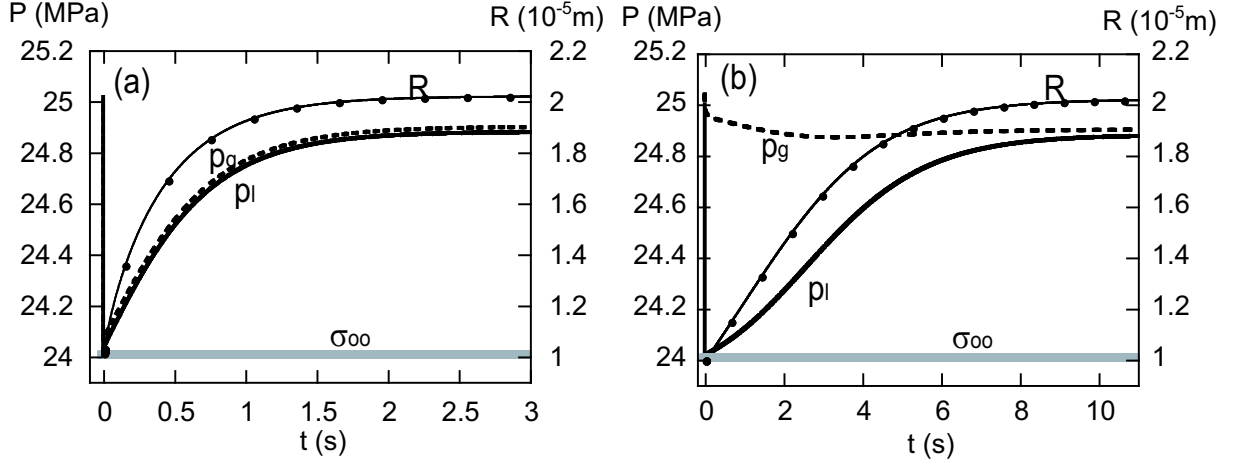


Figure 8: Pressure recovery in a bubbly magma in an elastic chamber after sudden unloading $\sigma_\infty = -1$ MPa. The initial condition is $p_l = p_g - 2\Sigma/R = 25$ MPa and $R = 10^{-5}$ m. The bubble radius on the right axis is plotted with a line-and-points. The stress and pressures on the left axis are plotted with a solid line for p_l , a dotted line for p_g , and gray line for σ_∞ . The system parameters are $\kappa_{gl} = 10^{-8}$ m².s⁻¹, the bubble number density is 10^{11} m⁻³, and $\eta_l = 50$ Pa.s for (a) and 10^6 Pa.s for (b). The others are the same as those for the basaltic system by [86].

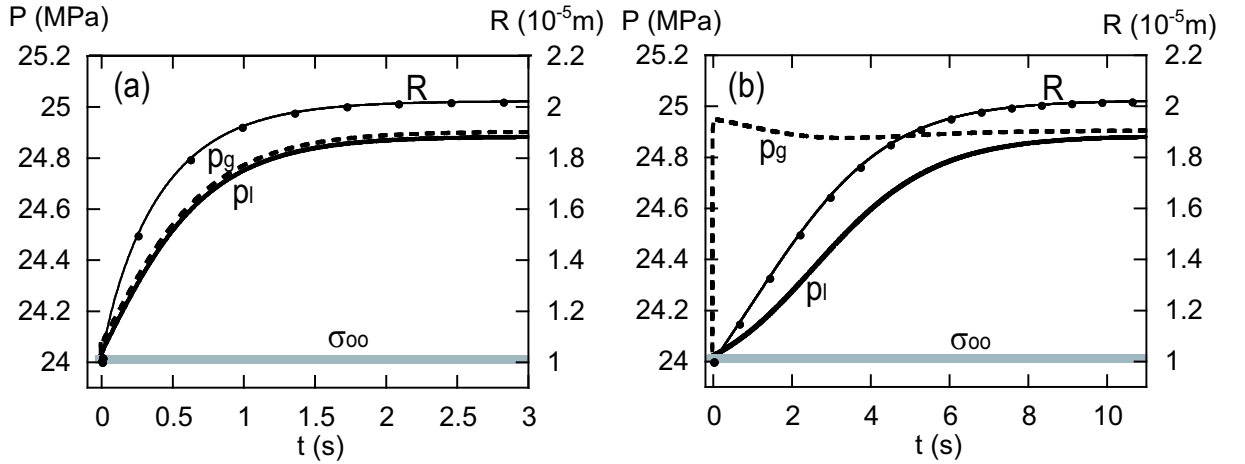


Figure 9: Similar to Figure 8, but the initial condition is $\sigma_\infty = p_l - p_o = p_g - 2\Sigma/R - p_o = -1$ MPa, with $p_o = 25$ MPa.

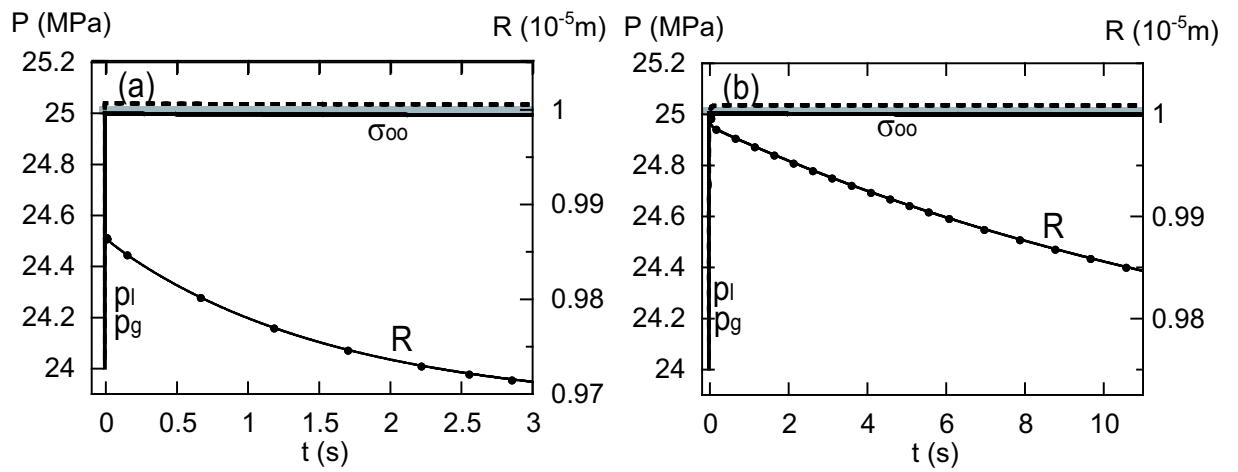


Figure 10: Similar to Figure 8, but the initial condition is $\sigma_{\infty} = 0$ and $p_l - p_o = p_g - 2\Sigma/R - p_o = -1$ MPa, with $p_o = 25$ MPa.

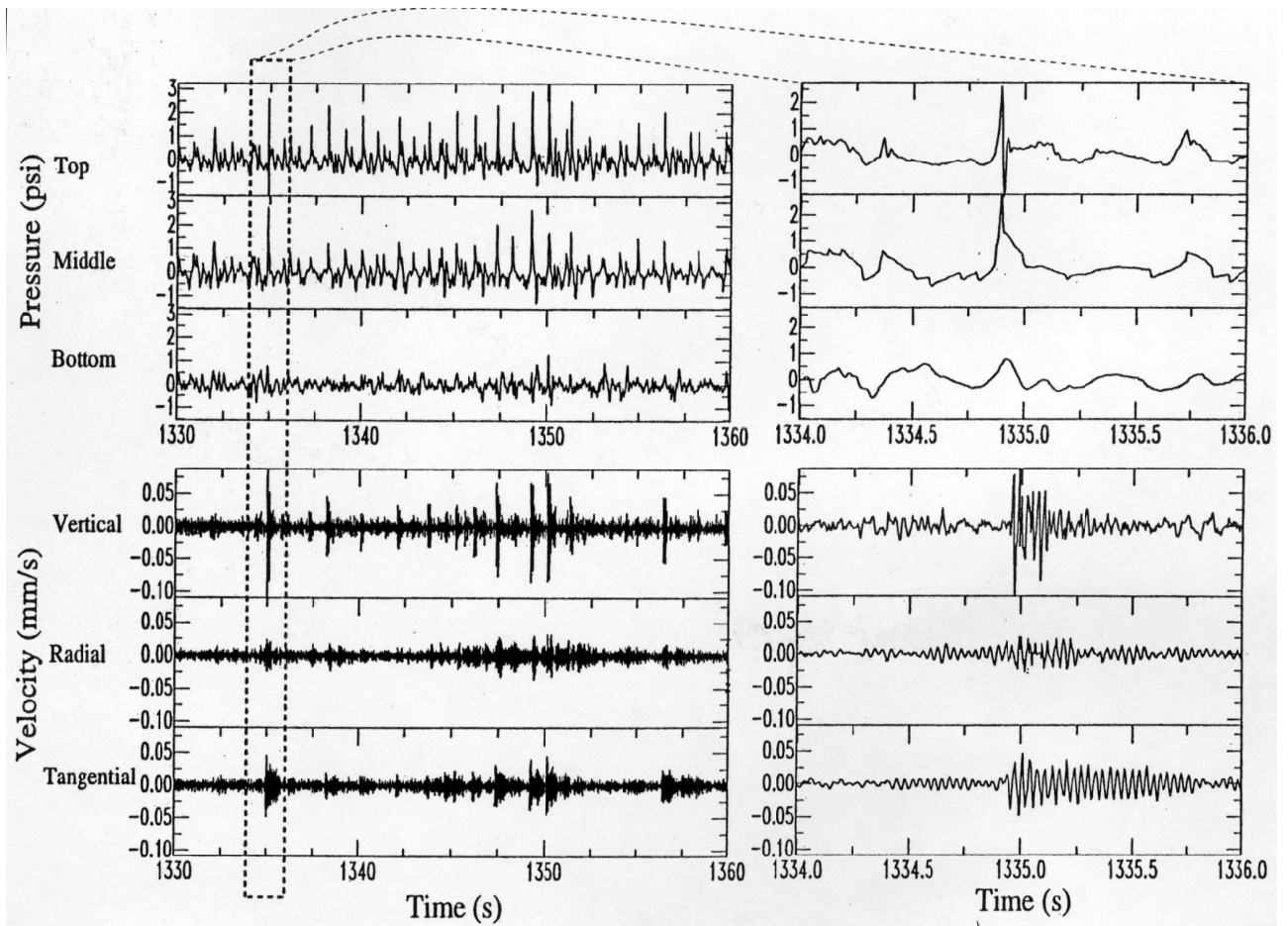


Figure 11: Simultaneous pressure records (high-pass filtered at 1 Hz) and seismic traces at Old Faithful geyser, Yellowstone. The geyser's eruptions are 2-5 min long with the interval between them ranging from 30-100 min. The figure shows a 30-s data about 27 min after the previous eruption and about 52 min before the next eruption. The conduit of the geyser is 22-m deep, where the bottom sensor was located. The bottom, middle and top sensors were connected 3 m apart. The seismic station was located at ~ 25 m from the geyser. The data show a direct correspondence between the pressure pulses and the seismic signals that follow them. ([40]FIG.3)

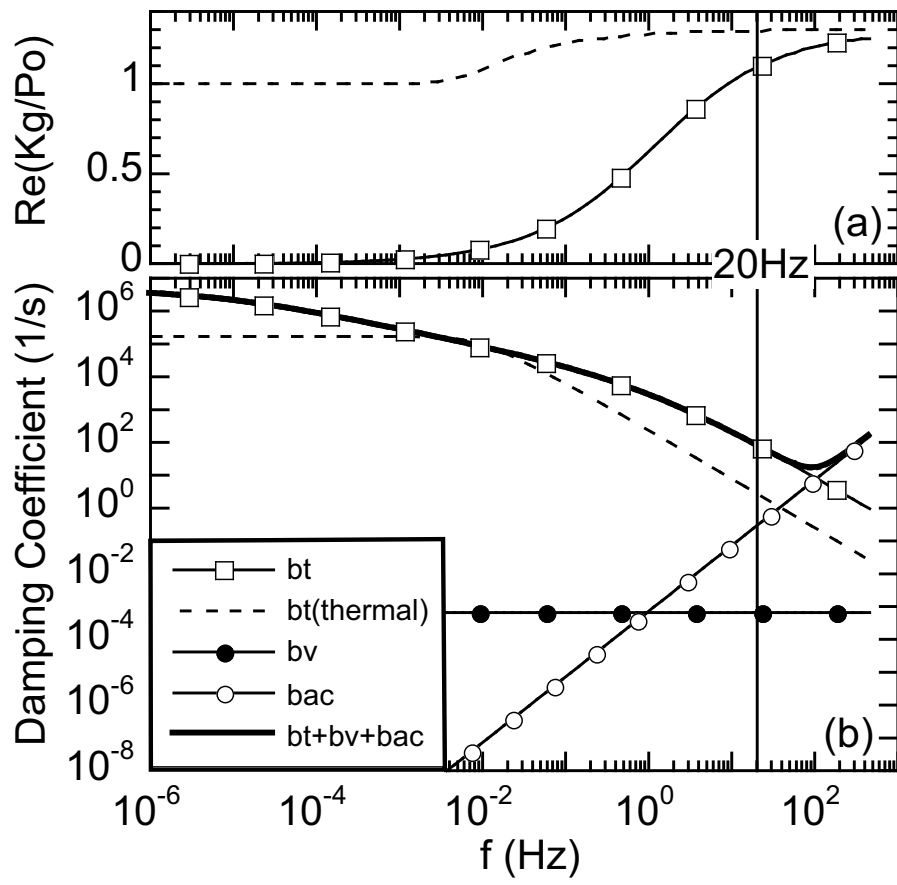


Figure 12: The bubble elasticity (a) and damping factors (b) for a single vapor bubble with radius 0.055 m at 380 K, 0.13 MPa (saturation pressure).

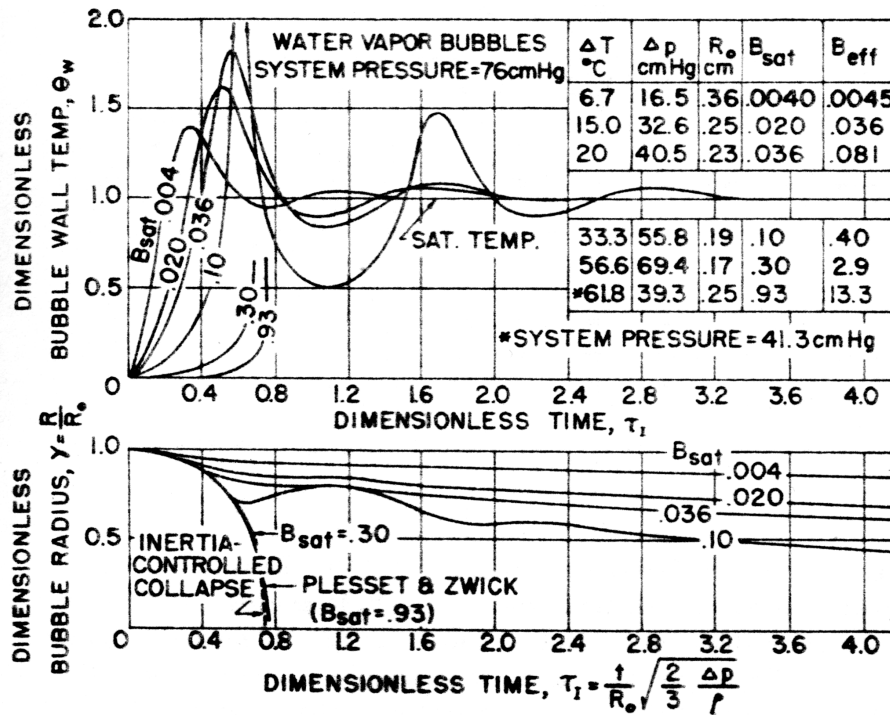


Figure 13: Variation of wall temperature and radius during collapse of water vapor bubbles. B_{sat} is the dimensionless parameter given by equation (35), which determines relative importance of the liquid inertia and the heat transfer. ([20] Fig.3)

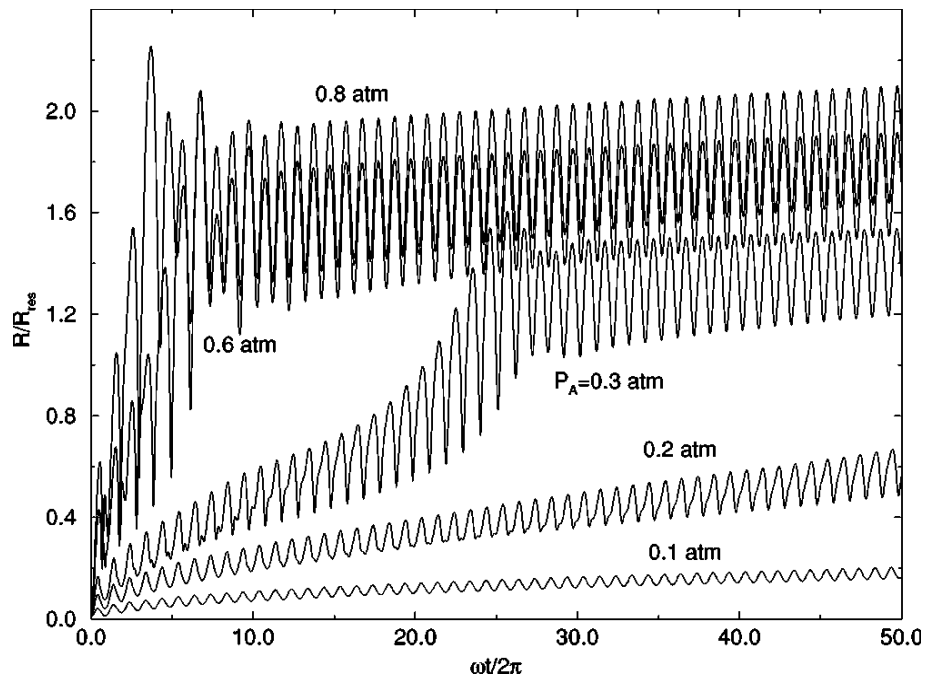


Figure 14: Growth of a vapor bubble by rectified heat transfer. Bubble radius normalized by the linear resonant radius $R_r = 2.71$ mm versus time for saturate water at 1 atm. The sound frequency is 1 kHz and the amplitude is attached to each profile. ([24] FIG.4)

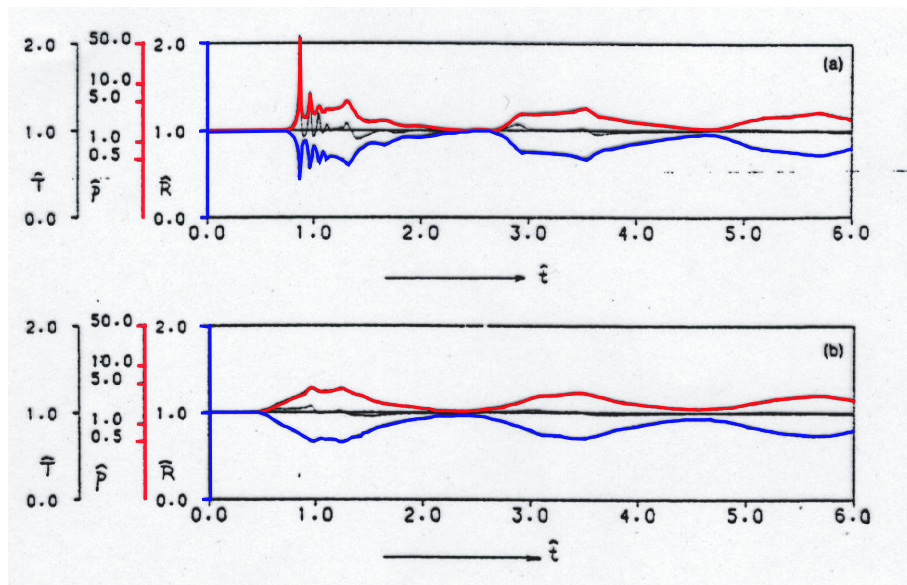


Figure 15: Change of bubble radius (blue lines) and pressure (red lines) in a spherical cloud of bubbles after a sudden pressure rise. The initial pressure and temperature are 3×10^4 Pa, 293 K, radii of the bubble and the cloud are 2.5×10^{-4} m and 3×10^{-2} , the void fraction is 3 %, and the pressure rise is 2.4×10^4 Pa. Values at the center (a) and at a half the radius from the center (b) are presented in dimensionless form (a unit of the dimensionless time corresponds to \sim ms). (modified from [67] Fig.9)